VISCOSITY MEASUREMENTS OF BULK METALLIC GLASS FORMING ALLOYS

Thesis by

Eric Bakke

In Partial Fulfillment of the Requirements

for the Degree of

Doctor of Philosophy

California Institute of Technology

Pasadena, California

1997

(submitted July 17, 1996)

To my parents,

who sparked imagination in a little boy a long time ago.

ACKNOWLEDGMENTS

I would like to acknowledge Professor William L. Johnson for giving me the opportunity to pursue my Ph.D. at Caltech. His strong intuition for physics and his ability to 'predict' what experiments are important have expedited my time here.

It goes without saying my many thanks to Dr. Ralf Busch, without whose input a large percentage of the work done in this thesis would not be complete. Our collaboration and friendship has proved very fruitful over the past few years, to which I am deeply indebted.

There are many people at Caltech who I would like to thank for their patience and friendship, and I will apologize beforehand if I forget to mention anybody. My thanks PO, Renato Camata, YJ, 'the lunch bunch', the machinists for their great help: Mike Gerfen (of infinite patience) and Joe Fontana, and many others.

I would like to thank the people at Tetrahedron Associates, Inc., for advice and insight to the workings of their product, along with some pleasant conversation.

Without the help of Matthew Urias of Mattco, the processing experiments certainly would have been tedious if not impossible.

My thanks goes to the people of Amorphous Technologies International for giving me the chance to consult and meet some of my goals, professional and personal, during my stay at Caltech.

I would like to thank Dr. Y. Tang and Chevron Corp., and Professor W. Goddard without whom, I would have never had the opportunity to attend Caltech.

My final, and deepest, thanks goes to my future wife and lifelong partner Kathy, who has put up with me at my worst and at my best since the beginning of this journey.

ABSTRACT

The viscosity of the $Zr_{46.75}Ti_{8.25}Cu_{7.5}Ni_{10}Be_{27.5}$ bulk metallic glass forming alloy in both the supercooled liquid and the equilibrium molten state was measured. Parallel plate rheometry and three-point beam-bending were used to measure the viscosity as a function of temperature in the supercooled liquid, and the technique of capillary flow was used in the molten state. The high thermal stability above the glass transition of this bulk metallic glass former with respect to crystallization allows measuring viscosities 120 K into the supercooled liquid region. Viscosity in the range from 10^{10} to 10^{6} poise has been measured using parallel plate rheometry, a region of viscosities that has not been previously accessible for supercooled metallic melts. The measurements were carried out with different heating rates between 0.0167 K/s and 1.167 K/s as well as isothermally. Using three-point beam bending, viscosity in the range from 10^{15} to 10^{8} poise has also been measured. These two methods, which involve completely different geometries for the measurement of flow, yielded consistent values for viscosity where their applicable regions overlap. The viscosity of the supercooled liquid of this bulk glass former, above the glass transition temperature, can be fit by a Vogel-Fulcher relation which exhibits a small Vogel-Fulcher temperature relative to the glass transition temperature. The values of viscosity measured by capillary flow above the liquidus temperature agree with the extrapolation of the Vogel-Fulcher relation to these temperatures. This bulk metallic glass

former exhibits strong glass behavior, similar to silicate glasses. The relatively high viscosity in the supercooled liquid and smaller Gibbs free energy difference compared to the crystal both favor bulk glass formation. This glass forming ability is directly related to the fragility index and the relaxation kinetics as measured by viscosity, as well as the critical cooling rate. Knowledge of the viscosity as a function of temperature is essential for shaping and molding, and has led to possible extended commercial applications of these novel materials which exhibit unique mechanical properties.

CONTENTS

List of Figures

Chapter 1:

Chapter 2:

Chapter 3:

Chapter 4:

Chapter 5:

Chapter 1:

INTRODUCTION

A glass is a solid formed by cooling (quenching) the liquid phase (melt) and 'freezing in' the liquid-like structure. This solid lacks any long range order, as opposed to the crystalline phases of the solid. A solid of this type containing a majority of one or more metal components and which exhibits metallic electrical conductivity is called a metallic glass. Metallic glass alloys were first obtained by liquid quenching by Duwez et al. [1] over 35 years ago. Since that time, many systems have been found that form glass from the liquid state. However, in order to form these systems, the cooling rate was limited to high values of 10^5 K/s or greater, and therefore the specimens had to be thin (< a few hundred microns) in at least one dimension. Later, by judicious choice of alloy compositions showing deep eutectic features, critical cooling rates down to 10^2 K/s or less were obtained and samples with dimensions of the order of millimeters could be formed [2]. In recent years, alloys with critical cooling rates of 10 K/s and as low as 1 K/s have been found, including those of the Zr-Ti-Cu-Ni-Be system [3]. One such alloy is $Zr_{46.75}Ti_{8.25}Cu_{7.5}Ni_{10}Be_{27.5}$. Casting of glassy samples greater than one centimeter in thickness samples are possible, and the term bulk metallic glass is now used to describe these new materials.

The metallic glass systems so far discovered are all metastable phases. In order to make a glass, the liquid must be cooled sufficiently fast from

the molten state above the liquidus temperature, T_{liq}, to the glass transition temperature, T_g, to avoid nucleation of crystalline phases. Once cooled below T_g in the glassy state, the atomic mobility is such that nucleation of crystals does not occur in reasonable time periods. Bulk metallic glasses with a high thermal stability can be undercooled with a cooling rate as little as 1 K/s. Upon reheating, these glasses have a large supercooled liquid region above the glass transition temperature [3,4]. Their stability enables thermophysical properties, such as specific heat capacity [5], diffusion [6], and in this study, viscosity, to be measured far into the supercooled region.

According to classical nucleation theory, the nucleation rate is determined by two factors; first, the decrease in atomic mobility as the temperature is lowered during quenching, and second, the free energy difference between the liquid and crystalline phases which provides a driving force for crystallization (Spaepen and Turnbull [7] and Uhlmann [8]). The rate of crystal nucleation as a function of temperature is then found from:

$$I \cong A\frac{T}{\eta(T)}\exp\left(-\frac{\Delta G^*}{kT}\right) \tag{1.1}$$

where $\eta(T)$ is the viscosity, T the temperature, k the Boltzman constant and A is a constant. ΔG^* is the activation energy for homogenous

nucleation of crystals from the liquid:

$$\Delta G^* = \frac{16\pi\sigma^3}{3\Delta G^2} \tag{1.2}$$

where σ is the interfacial surface tension and ΔG is the Gibbs' free energy difference between the liquid and the crystal. This model was developed for pure elements or for the polymorphic case. The crystallization of the Zr-Ti-Cu-Ni-Be system involves composition fluctuations or phase separation [9], so the entire nucleation rate cannot be described by eq. 1.1. However, the viscosity dependence with temperature through the undercooling is an important factor on how nucleation rates proceed and in the critical cooling rate required for glass formation. Upon cooling a metallic melt, mobility of the atoms decreases rapidly as the liquid passes through the glass transition region. This decrease in mobility corresponds to an increase of viscosity. The viscosity of $Zr_{46.75}Ti_{8.25}Cu_{7.5}Ni_{10}Be_{27.5}$ varies from values of order 50 poise at T_{liq} (1100 K) to 10^{13} poise at 595 K (which roughly corresponds to T_g for very small heating rates). By cooling from the molten state to below T_g, such a large change in viscosity (eleven orders of magnitude) results in the kinetic freezing of the liquid phase and ultimately halts any further crystallization on reasonable timescales.

By using different cooling rates, different amounts of excess enthalpy can be 'quenched-in' the glass phase. The glassy phase will subsequently undergo relaxation upon reheating to temperatures near, but below, Tg. This relaxation is accompanied by the release of the stored excess enthalpy. The equilibrium atomic configuration of the homogeneous liquid is ultimately approached during this process of minimizing of stored enthalpy [10]. The time for an undercooled liquid to reach configurational equilibrium, the relaxation time, depends upon the atomic mobility, i.e., the viscosity. At a viscosity of 10^{13} poise, the relaxation time to equilibrium is on the order of minutes. The relaxation time scales roughly with viscosity, so that at 10^{10} poise, it is about one second, and at 10^{20} poise relaxation times are of the order of 300 years! Once the temperature is lowered such that the viscosity is above 10^{16} poise, the rate of atomic reconfiguration becomes so small that equilibrium is not reached in typical laboratory time scales. Viscosity of up to 10^{16} poise can be measured by patiently waiting to reach the configurational equilibrium condition on laboratory time scales (almost one month).

Forming a bulk metallic glass with lower cooling rates results in a glass which is nearer the equilibrium configuration. When one measures a property of the glass at a given temperature, the equilibrium value of that property is attained in a shorter time period for the more relaxed glass. The thermal processing history of the glass will thus affect the properties of the glass. This concept can be applied if one is measuring a property

under different constant heating rate conditions. The property measured will have different values at a given temperature for different heating rates. At slow heating rates, the value of a physical parameter will approach the equilibrium value more closely than at higher heating rates. When relaxation times become smaller than the time scale for a measurement, the measured values become independent of heating rate and will be characteristic of an equilibrium configuration. As such, both history and temperature must be defined when discussing the properties of a glass.

The glass transition temperature, T_g, itself has different values for different heating rates. The glass transition can be measured using several different methods. One method is differential scanning calorimetry (DSC). The glass transition is exhibited through the increase of the value of the specific heat capacity of the glass from a value near that of the crystal to a value characteristic of the supercooled liquid [5] (see Fig. 1.1). Closer examination of the specific heat with temperature shows that, when using a finite heating rate, there is a continuous change in the measured heat capacity. The apparent glass transition shifts to higher temperatures with higher heating rates. In effect, the glass transition has an onset and a completion value. With higher heating rates, the glass transition onset and completion temperatures are shifted to higher values. The glass transition temperature is a function of the degree of relaxation as mentioned above, and can itself be related to the viscosity. For the

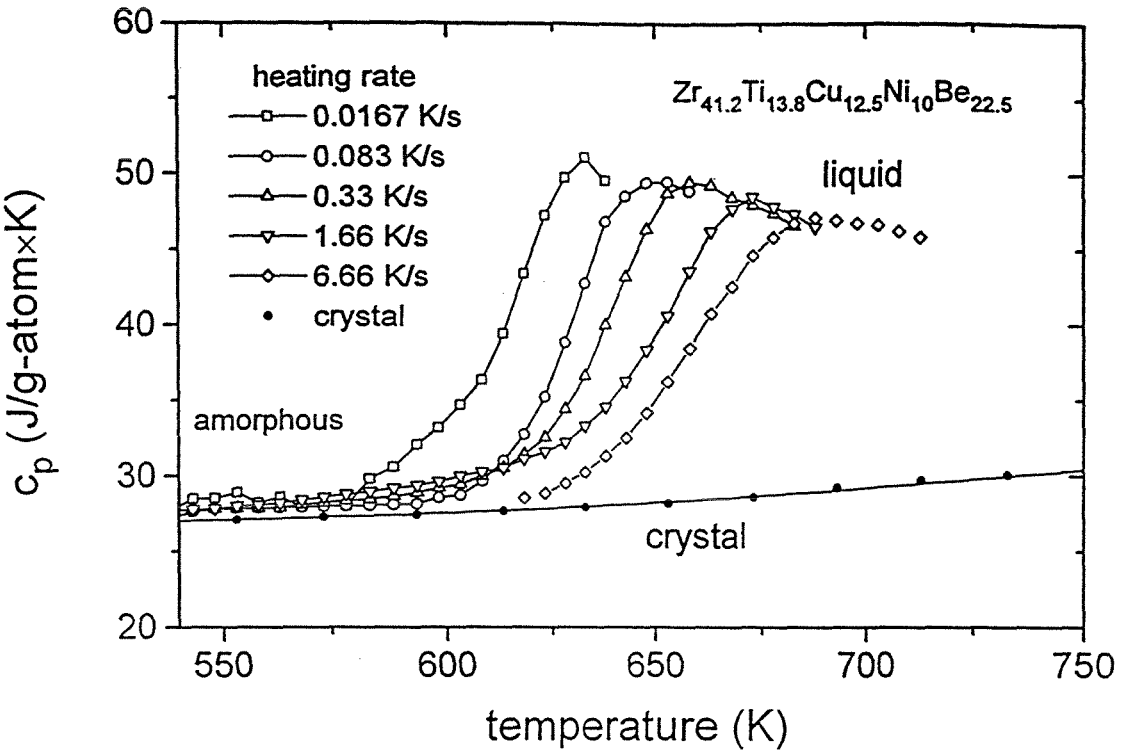

Fig. 1.1. Specific heat capacity as a function of temperature for different heating rates as measured by Differential Scanning Calorimetry (DSC) for the $Zr_{41.2}Ti_{13.8}Cu_{12.5}Ni_{10}Be_{22.5}$ alloy. Reproduced from ref. 5.

purposes of this study, I will refer to the glass transition temperature, T_g, as the temperature at which the viscosity has a value of 10^{13} poise. Of course, this will in fact depend on the thermal history of the sample.

The viscosity of bulk glass forming alloys varies over almost twenty orders of magnitude as a function of temperature from the equilibrium melt (50 poise) to the glassy state at room temperature (> 10^{20} poise). Such a large range of viscosity cannot be measured using a single experimental method, and equilibrium viscosities above 10^{16} poise are very difficult to measure at all. In order to measure the viscosity over many orders of magnitude, different methods are used. In this study, I will report on three different methods to measure the viscosity. These are: the parallel plate method, three point bending, and the capillary flow technique.

Viscosity of metallic glasses in the supercooled liquid region has been previously measured, for example by Chen and Turnbull [11], Tsao and Spaepen [12], and Volkert and Spaepen [13]. These investigators used tensile creep of thin melt-spun ribbons or wires for measuring viscosity (for example, see Fig. 1.2). By loading the sample in tension and measuring the resulting plastic deformation with time, the viscosity can be found from:

$$\eta = \frac{\sigma}{3\dot{\varepsilon}} \tag{1.3}$$

where σ and $\dot{\varepsilon}$ are the tensile stress and the strain rate, respectively. These experiments were performed under continuous heating and isothermal conditions to observe the relaxation effects described above.

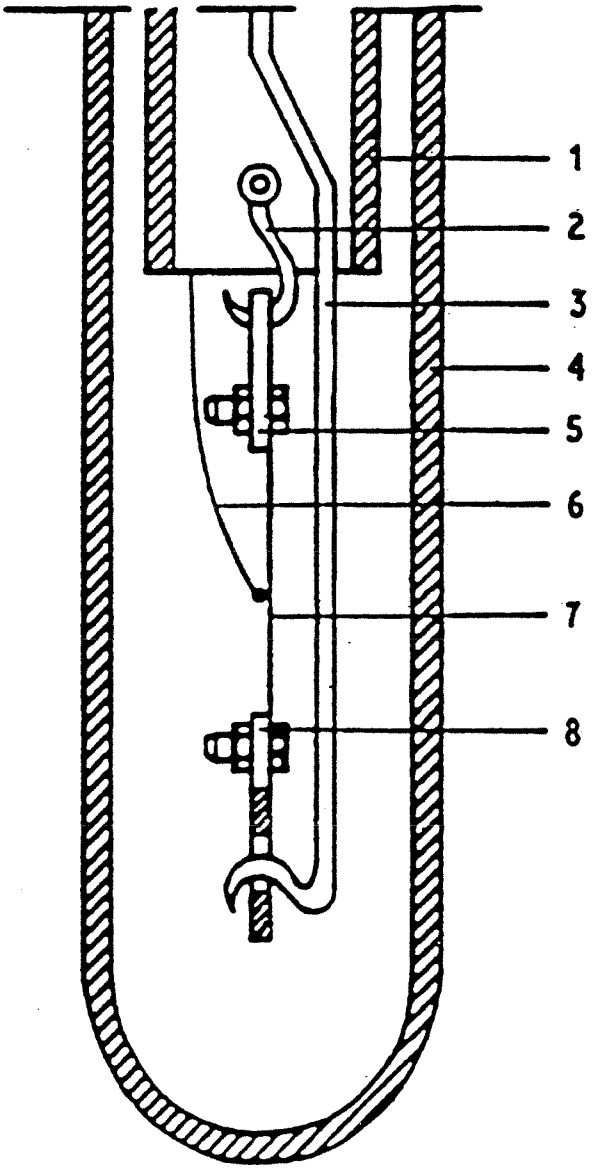

Schematic diagram of the silica glass assembly for creep measurements of the Heraeus TMA 500 dilatometer. 1, supporting silica glass tube; 2, silica glass hook; 3, silica glass rod with hook at end for applying load and connecting moving grip to LVDT-core; 4, protecting silica glass tube; 5, stationary grip of the Invar alloy; 6, thermocouple; 7, specimen; 8, moving grip of Invar alloy. Measurements are carried out in inert atmosphere with Ar as purging gas.

Fig. 1.2. Tensile creep apparatus used to measure viscosity. Reproduced from ref. 18.

The viscosity of melt-spun ribbons were also measured with a three-point bending apparatus under continuous heating [14]. However, the viscosities were measured not far above the glass transition temperature (Fig. 1.3). The onset of crystallization halted further measurement into the supercooled liquid. As such, the viscosity of the supercooled liquid could only be obtained in a very narrow temperature interval where relaxation effects can make interpretation of the data difficult. Another method used to measure viscosity is internal friction or dynamic mechanical analysis (see ref. [15] for example). In this method, the sample was subject to a constant force and a superimposed oscillating force. By measuring the storage and loss modulus as a function of temperature and frequency, the viscosity as a function of temperature can be measured.

The strong temperature dependence of the viscosity as measured by these methods could be fitted well with a Vogel-Fulcher equation:

$$\ln \eta = A + B/T\text{-}T_o \tag{1.4}$$

where A, B, and T_o are fitting parameters. The relatively narrow temperature interval of the viscosity data yielded T_o values close to the measured T_g values. This type of viscosity dependence with temperature is consistent with metallic glasses having a higher critical cooling rate and a narrow temperature interval for crystallization of the supercooled liquid. With the advent of bulk metallic glass with critical cooling rates of 10 K/s or less, the thermal stability of the supercooled liquid is increased, and viscosity measurements can be extended further into this previously

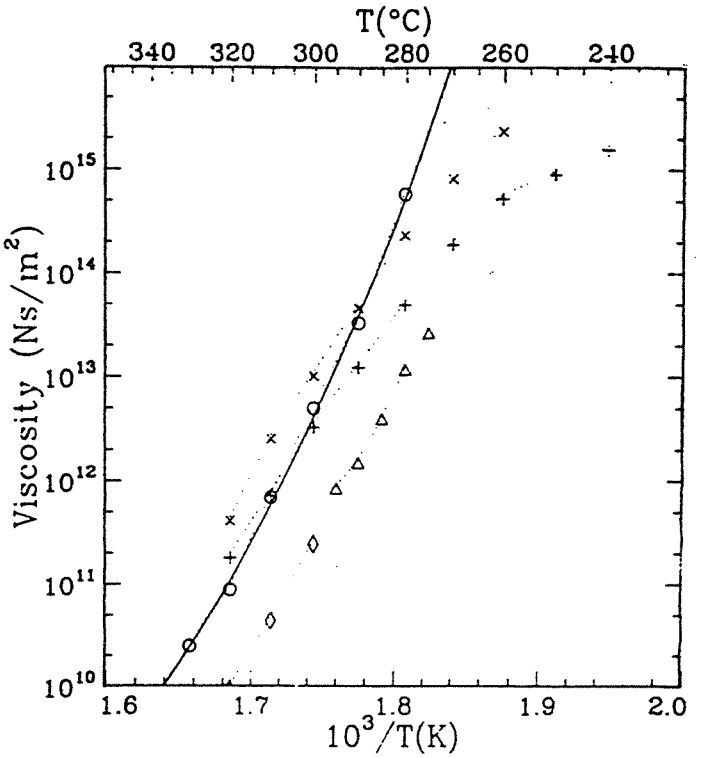

Fig. 1.3. Tensile creep viscosity measurements.

○ equilibrium viscosity of $Pd_{40}Ni_{40}P_{19}Si_1$
△ equilibrium viscosity of $Pd_{40}Ni_{40}P_{20}$
◇ equilibrium viscosity of $Pd_{48}Ni_{32}P_{20}$
\+ isoconfigurational viscosity of $Pd_{40}Ni_{40}P_{19}Si_1$ equilibriated at 583 K
× isoconfigurational viscosity of $Pd_{40}Ni_{40}P_{19}Si_1$ equilibriated at 563 K

Reproduced from ref. 19.

unmeasured region for metallic glasses. Also, different types of measurements of viscosity other than the ones mentioned above can now be applied (parallel plate in this study).

In order to process and form bulk metallic glass by such methods as casting, die casting, molding and extrusion, knowledge of the viscosity as a function of temperature and time is essential. Using the concepts developed above, relaxation effects, and equilibrium viscosity, the parameters required to process a bulk metallic glass by molding or extrusion can be determined. Knowing the viscosity of the melt is important for any casting process. By freezing in the liquid phase during solidification, shrinkage during casting is minimized, and net shaping of components can be achieved.

The processes above allow commercial application of bulk metallic glasses in fabrication of high quality net shape metal components. The mechanical properties of these glasses are unique among the metals used in industry. These materials exhibit high strength [16] and hardness, fatigue resistance, fracture toughness [17] and corrosion resistance. Using the processing techniques developed in this, specifically molding, the commercial application of bulk metallic glass have been extended beyond casting net shapes from the melt to viscous forming operations at lower temperatures. Such processing methods are presently used for forming thermoplastics and have not been previously applied to metals. The time, temperature, and pressure conditions necessary for forming the glass in

the desired shape have been defined by the preliminary molding experiments performed in this work. Equipment for carrying out such operations has also been developed.

References

[1] P. Duwez, R. H. Willens, and W. Klement, J.Appl. Phys. **31**, 1137 (1960).

[2] W. L. Johnson, *Metals Handbook*, 10th Edn., Vol. 2 ASM International, Metals Park, OH, 812 (1990).

[3] A. Peker and W. L. Johnson, Appl. Phys. Lett. **63**, 2342 (1993).

[4] A. Inoue, T. Zhang, and T. Masumoto, Mater. Trans. JIM **31**, 17 (1990).

[5] R. Busch, Y. J. Kim, and W. L. Johnson, J.Appl. Phys. **77**, 4039 (1995).

[6] U. Geyer, S. Schneider, W. L. Johnson, Y. Qiu, T. A. Tombrello, and M. P. Macht, Phys. Rev. Lett. **75**, 2364 (1995).

[7] F. Spaepen, and D. Turnbull, *Rapidly Quenched Metals*, Vol. II (eds N. J. Grant, and B. C. Giessen). MIT Press, Boston, 205 (1976).

[8] D. R. Uhlmann, J. Non-Cryst. Solids **17**, 337 (1972).

[9] R. Busch, S. Schneider, A. Peker, and W. L. Johnson, Appl. Phys. Lett. **67**, 1544 (1995).

[10] R. W. Douglas, Brit. J. Appl. Phys. **17**, 435 (1966).

[11] H. S. Chen and D. Turnbull, Journ. Chem. Phys. **48**, 2560 (1968).

[12] S. S. Tsao and F. Spaepen, Acta metall. **33**, 881 (1985).

[13] C. A. Volkert and F. Spaepen, Acta metall. **37**, 1355 (1989).

[14] K. Russew and L. Stojanova, Mat. Sci. and Eng. **A123**, 59 (1990).

[15] W. Myung, S. Kim, D. Jang, H. Okumura, A. Inoue, and T. Masumoto, J. Non-Cryst. Solids **150**, 406 (1992).

[16] H. A. Bruck, T. Christman, A. J. Rosakis, and W. L. Johnson, Script. Met. **30**, 429 (1994).

[17] D. Conner, A. Rosakis, and W. L. Johnson, (unpublished research).

[18] K. Russew, et al., J. Mat. Sci. **27**, 3565 (1992).

[19] C. A. Volkert and F. Spaepen, Mat. Sci. Eng. **97**, 449 (1988).

Chapter 2:

VISCOSITY MEASUREMENTS

2.1 Qualitative Description of Flow

When stress is applied to a material, the material responds elastically or viscously, or both with time. Materials also exhibit other behavior, e.g., anelasticity, which is beyond the scope of this study. Typically, at some fixed temperature T:

$$\tau = f(\varepsilon, \dot{\varepsilon}, t) \tag{2.1}$$

where τ = shearing stress, ε = strain and $\dot{\varepsilon} = \frac{\partial \varepsilon}{\partial t}$ = rate of strain. These are written as tensors of rank two for three dimensions. For an ideal elastic body, the strain is proportional to the stress. Once the stress is removed, the body returns to its original shape. An ideal viscous body exhibits flow, and the body remains in its final configuration once the stress is removed. The rate of flow is a function of the stress, and there are two types, viscous shear flow and flow defined by the bulk viscosity [1]. Bulk viscosity is related to the lag time for filling free volume of a liquid during hydrostatic compression or decompression. Its elastic counterpart is bulk modulus (or compressibility). In this study, the term viscosity is used only to describe shear flow. For Newtonian fluids, the coefficient of viscosity is constant

with stress:

$$\tau(t) = f(\dot{\varepsilon}, t) = \eta \dot{\varepsilon}(t) \tag{2.2}$$

where η is the viscosity.

In a three-dimensional coordinate system x, y, and z:

$$\tau_{yx} = -\eta \frac{\partial v_x}{\partial y} \tag{2.3}$$

or in tensor notation:

$$\tau_{ji} = -\eta \frac{\partial v_i}{\partial x_j} \tag{2.4}$$

where $v_i = \frac{\partial x_i}{\partial t}$. This definition of viscosity, which relates the stress tensor to the rate of deformation tensor, can be visualized using Fig. 2.1. The surface at y=0 acquires a certain amount of x-momentum; this layer in turn imparts some of its momentum to the adjacent layer immediately above it and so on. τ_{yx} may be interpreted as the viscous flux of x-momentum transfer in the y-direction.

In a viscosity measurement, a force is applied to the sample and the resulting deformation is measured as a function of time. The apparent viscosity can then be expressed as:

$$\eta = (1/f)F/v \tag{2.5}$$

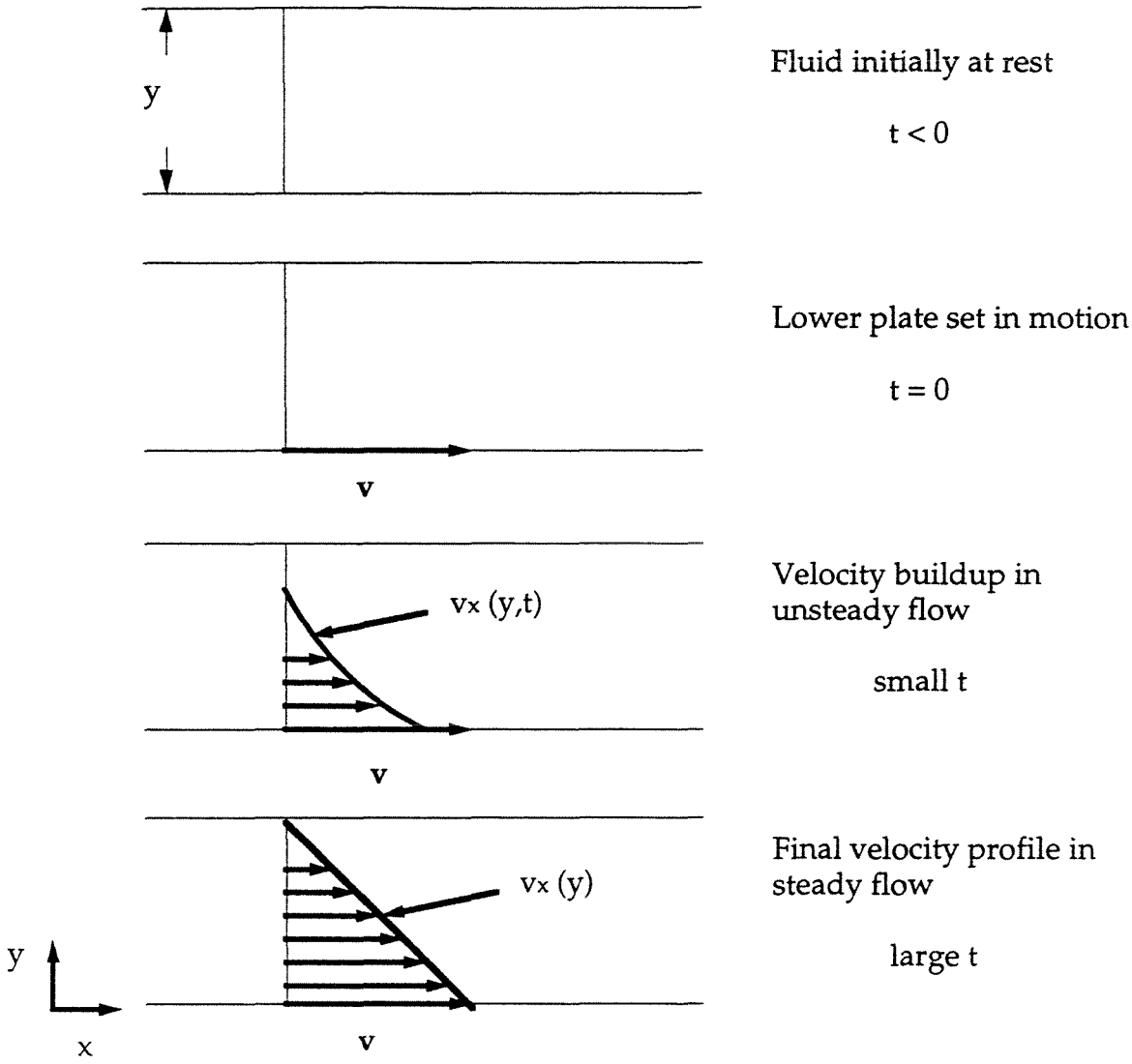

Fig. 2.1. Buildup to steady laminar velocity profile for a fluid between two plates. Reproduced from Ref. 9.

where F is the force, v is the measured velocity of deformation, and f is a form factor for the different geometries of flow for the different measurements.

2.2 Parallel Plate Rheometry

In parallel plate rheometry, the viscosity is found by measuring the deformation of a cylindrical sample with time under an axial load between two plates. This method can be applied to materials with a viscosity in the range from roughly 10^{10} to 10^{3} poise. For metallic glasses, this range of viscosity is difficult to measure using other methods. Two cases can be considered, one in which the material completely fills the space between the plates and the other where the material never completely fills the space (see Fig. 2.2). For the parallel plate measurements done in this study, all viscosity measured was of the former case. Parallel plate rheometry has been used previously to measure viscosity of several materials, including polymers [2] and silicate glasses [3]. For the first time, this method has been applied to a bulk metallic glass forming system.

In order to obtain a relation in which the measured viscosity depends only on the force and the displacement of one plate with respect to the other as a function of time, the general equation for flow must be simplified considerably. The general equation of motion for a Newtonian fluid of viscosity η is:

$$\rho\frac{\partial\bar{\mathbf{v}}}{\partial t}+\rho\bar{\mathbf{v}}\cdot\nabla\bar{\mathbf{v}}=-\nabla p+\eta\nabla^{2}\bar{\mathbf{v}}+\frac{1}{3}\eta\nabla\nabla\cdot\bar{\mathbf{v}}+\rho\bar{\mathbf{g}} \qquad (2.6)$$

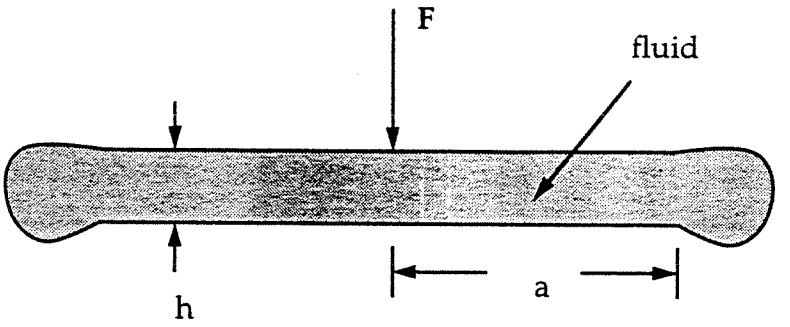

Case 1

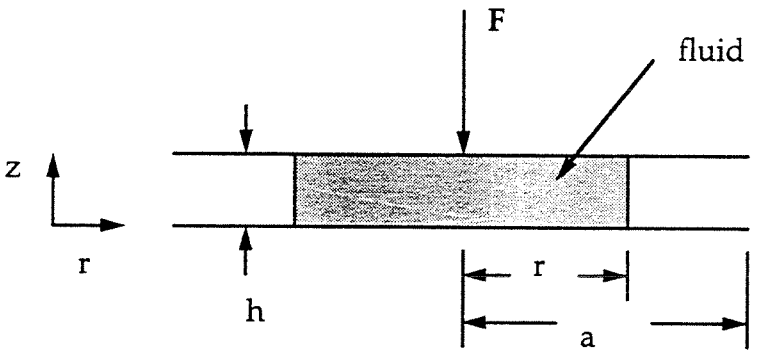

Case 2

Fig. 2.2. The two sample geometries for parallel plate rheometry.

where $\bar{\mathbf{v}}$ is the velocity vector of the fluid, ρ the density, p the pressure, and $\rho\bar{\mathbf{g}}$ the gravitational body force, which can be ignored compared to the forces used for the measurements in this study. For an incompressible fluid, $\nabla \cdot \bar{\mathbf{v}} = 0$. The velocities used in this experimental method are small (less than 2.5 X 10^{-3} mm/s in my case) and square terms of $\bar{\mathbf{v}}$ can be ignored. The equation of motion is then:

$$\rho \frac{\partial \bar{\mathbf{v}}}{\partial t} = -\nabla p + \eta \nabla^2 \bar{\mathbf{v}} \tag{2.7}$$

In cylindrical coordinates, the equation is written in component form:

$$-\frac{\partial p}{\partial r} + \eta \nabla^2 v_r = \rho \frac{\partial v_r}{\partial t} \tag{2.8}$$

$$-\frac{1}{r}\frac{\partial p}{\partial r} + \eta \nabla^2 v_\theta = \rho \frac{\partial v_\theta}{\partial t} \tag{2.9}$$

$$-\frac{\partial p}{\partial r} + \eta \nabla^2 v_z = \rho \frac{\partial v_z}{\partial t} \tag{2.10}$$

With the ends of the specimen cylinder in contact with the parallel plates, and with the further assumption that the plate separation h is small compared with the radius R of the specimen, boundary conditions can be

imposed at $z = 0$ and $z = h$. Also, the following assumptions can be made: $v_\theta = 0$ (circular symmetry, no angular velocity)

$v_z = 0$ (as long as h is small compared to R)

$v_r = 0$ at $z = 0$ and $z = h$ (no slippage at the plates).

The equation of motion is then reduced to:

$$\frac{\partial p}{\partial r} = \eta \frac{\partial^2 v_r}{\partial z^2} \tag{2.11}$$

This equation is similar to flow through a pipe, where there is a pressure gradient forcing material from one end to the other and the velocity profile is parabolic through the cross section. The rest of the derivation involves imposing the boundary conditions and conservation of mass as flow occurs through differential elements of the surface. The rest of the derivation is found in Appendix I, and I will summarize these results below. If the sample is smaller than the radius of plates and the volume of material between them is constant, then:

$$F = -\frac{3\eta V^2}{2\pi h^5}\frac{dh}{dt} \tag{2.12}$$

where V is the volume of the sample, F is the force applied to the plates, h is the height, and dh/dt is the rate of change of the height.

For the case where the sample is larger than the plates:

$$F = -\frac{3\pi\eta a^4}{2h^3}\frac{dh}{dt} \tag{2.13}$$

where a is the radius of the plates.

Equation 2.13 can be rearranged:

$$\eta = -\frac{2Fh^3}{3\pi a^4 \, dh/dt} \tag{2.14}$$

By applying a constant force, and then measuring the height and the slope of the height with time, the viscosity can be found from eq. 2.14.

2.3 Flexure

Another method used to measure viscosity is flexure or three-point beam-bending. Here, a load is applied to the center of a beam of uniform cross-section supported on both ends, Fig. 2.3. By measuring the deflection of the center of the beam with time, the viscosity can be derived. Viscosity in the range from 10^{15} to 10^{8} poise can be measured. The method of three-point beam-bending has been used to measure the viscosity of silicate glasses [4]. Using this method, we have measured the viscosity of $Zr_{46.75}Ti_{8.25}Cu_{7.5}Ni_{10}Be_{27.5}$ in a region from 10^{15} to 10^{9} poise. Since there is an overlap in the range of viscosity covered by parallel plate rheometry

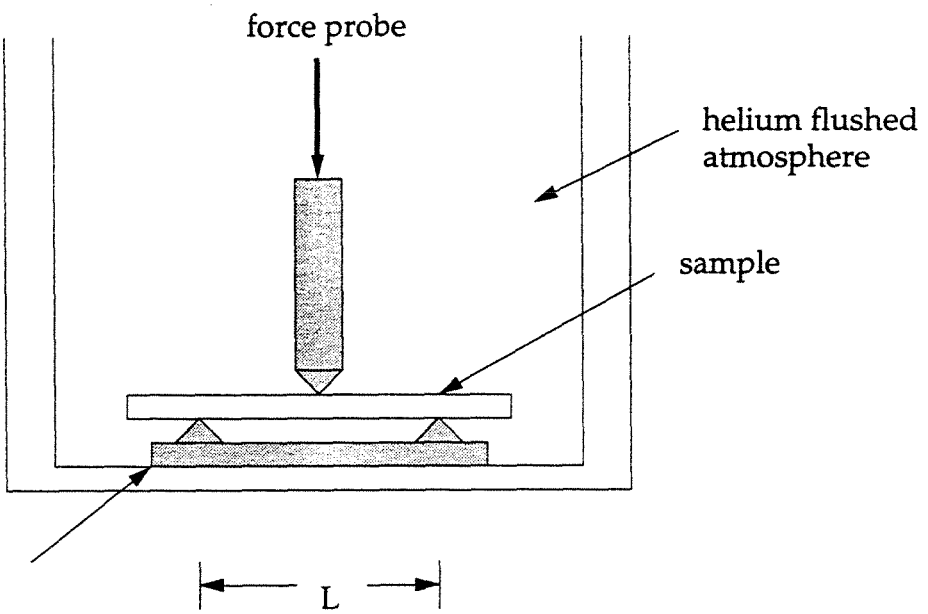

Fig. 2.3. Schematic diagram for three point bending or flexure.

and beam-bending, each method can verify the experimental accuracy of the other for this region. Both of these methods yielded consistent results for the measurement of viscosity in the region of overlap.

The viscosity in Pa • s can be found using the following equation (Hagy [4], Trouton [5] and Reiner [6]):

$$\eta = \frac{g L^3}{144 I_c v}\left[M + \frac{5\rho A L}{8}\right] \tag{2.15}$$

where g is the gravitational constant (m/s^2), I_C the cross-section moment of inertia (m^4), v the midpoint deflection rate (m/s), M the applied load (kg), ρ the density of the glass (kg/m^3), A the cross-sectional area (m^2), and L the support span (5.08×10^{-3} m for our apparatus). The derivation for equation 2.15 can be found in Appendix II.

2.4 Capillary Flow

The viscosity of the melt can be measured using the capillary flow method [7]. Here, the liquid is drawn up through a capillary by surface tension, hydrostatic pressure, or externally applied pressure. By measuring the time for a volume of liquid to rise through a capillary, the viscosity can be found. When one end of the capillary is introduced into the melt (see Fig. 2.4), the relation for the velocity of penetration in a capillary for

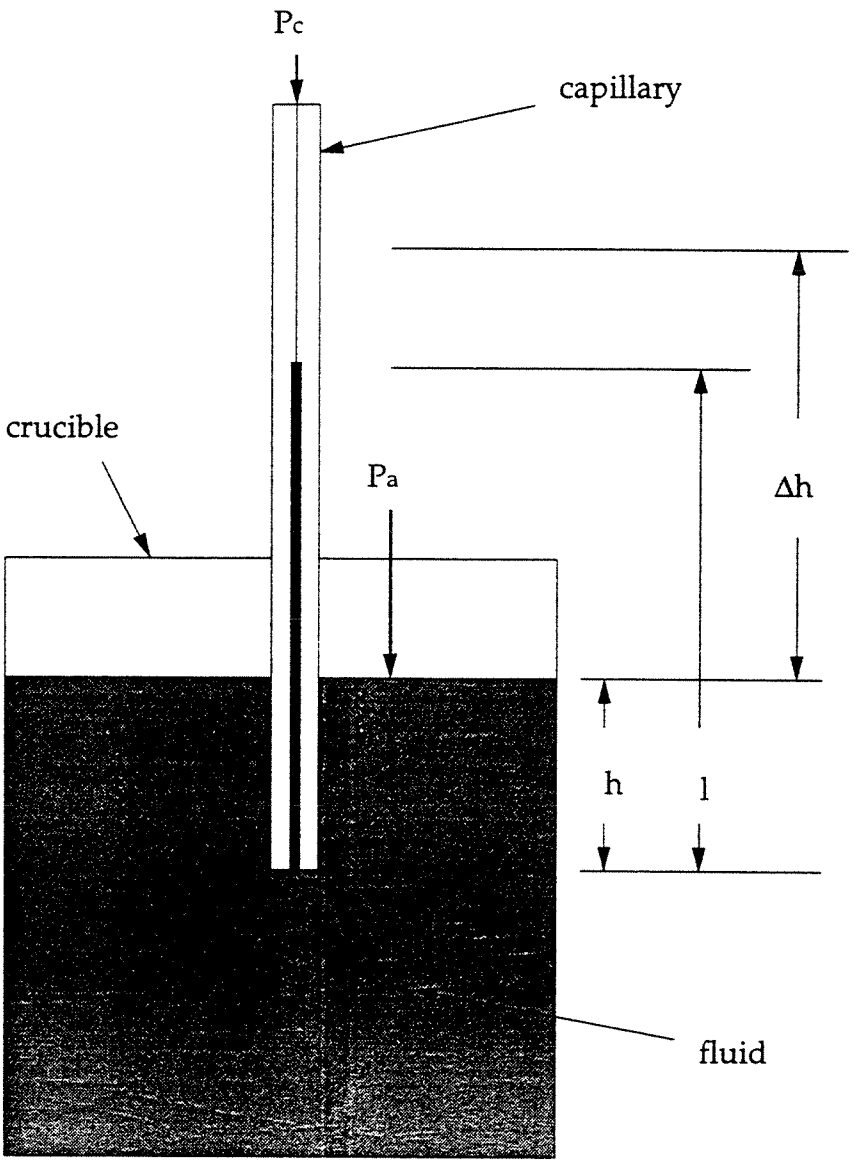

Fig. 2.4. Schematic diagram for capillary flow measurements.

laminar (non-turbulent) flow is:

$$\frac{dl}{dt} = \frac{\sum P \times (r^2 + 4\varepsilon r)}{8\eta l} \tag{2.16}$$

where ε is the coefficient of slip, r the radius of the capillary, and l the height above the surface of the melt. The coefficient of slip is related to the wetting of the capillary by the liquid and is close to zero for liquids which do wet the capillary. This is material dependent, and for the Zr-Ti-Cu-Ni-Be systems at the melting temperature with a quartz capillary, the wetting angle is less than 20°. The sum of the pressures are due to:

1. The pressure differential between the capillary and the pressure at the surface of the melt , $P_a - P_c$

2. Hydrostatic pressure, ρgh

3. Capillary pressure, P_S, defined below:

$$P_s = \frac{2\gamma}{r}\cos\theta \tag{2.17}$$

where γ is the surface tension and θ the wetting angle. If the pressure is the same at both ends of the capillary, and ρgh can be neglected if the capillary is not immersed deeply into the liquid, then viscosity can be

found from the following:

$$\frac{dl}{dt} = \frac{r}{\eta}\frac{\gamma}{4l}\cos\theta \tag{2.18}$$

where γ is the surface tension, r is the radius, $\cos\theta$ is the wetting angle, and η the viscosity. Here, the surface tension is the sole driving force causing flow through the capillary. Using this case, the surface tension is found from:

$$\Delta h = \frac{2\gamma}{r\rho g}\cos\theta \tag{2.19}$$

where Δh is the final height of the rise of the liquid. In this study, I will report only preliminary data, as a more extensive investigation of capillary flow is being performed by A. Masuhr and will be the subject of future publications [8].

Each of the three methods of measuring viscosity discussed above are obtainable only in certain regions. The regions of viscosity that can be measured by parallel plate and three-point bending cover twelve orders of magnitude themselves and overlap, but are removed from the capillary flow measurements by at least two orders of magnitude. This region must be measured by using some other technique, perhaps rotating cylinders. There are considerable technical difficulties to be overcome in capillary flow measurements, the primary one being the onset of crystallization

induced by heterogeneous nucleation. However, there is no reason to assume that the viscosity does not smoothly vary with temperature as the material remains in liquid phase throughout all of these regions. The viscosity is a continuous function with temperature. The data measured should follow the same overall viscosity function, provided equilibrium of the liquid has been achieved. By plotting the data from the various experiments, a single functional form of the viscosity with temperature can be found.

References

[1] S. M. Karim and L. Rosenhead, Revs. Mod. Phys. **24**, 108 (1952).

[2] G. J. Diennes and H. F. Klemm, Appl. Phys. **17**, 458 (1946).

[3] S. J. Wilson and D. Poole, Mat. Res. Bull. **25**, 113 (1980).

[4] H. E. Hagy, Jour. Am. Ceram. Soc. **46**, 93 (1963).

[5] F. T. Trouton, Proc. Roy. Soc. (London) **77**, 426 (1906).

[6] M. Reiner, *Rheology*, Vol. 1 (ed F. R. Eirich), Academic Press, New York, 9 (1956).

[7] E. W. Washburn, Phys. Rev. **17**, 273 (1921).

[8] A. Masuhr, R. Busch, E. Bakke, and W. L. Johnson, (unpublished research).

[9] R. B. Bird, W. E. Stewart, and E. N. Lightfoot, *Transport Phenomena*, John Wiley & Sons, New York, 4 (1960).

Chapter 3:

EXPERIMENTAL TECHNIQUES AND RESULTS

Amorphous $Zr_{46.75}Ti_{8.25}Cu_{7.5}Ni_{10}Be_{27.5}$ alloys were prepared from a mixture of the elements of purity ranging from 99.5% to 99.9% by induction melting and subsequent water quenching in 6.35 and 10.0 m m inner diameter silica tubes. Cylindrical samples were then cut from the 6.35 mm rod for use in parallel plate rheometry. Beams of rectangular cross-section were cut from the 10 mm rod for beam-bending. For both methods, the experimental apparatus used was a Perkin-Elmer Thermal Mechanical Analyzer (TMA 7). The experimental details of the capillary flow method will be the main topic in another publication and I will only discuss preliminary results here.

To study the viscosity from 10^{10} to 10^{6} poise of $Zr_{46.75}Ti_{8.25}Cu_{7.5}Ni_{10}Be_{27.5}$ as a function of temperature in the supercooled liquid, parallel plate rheometry was used. Quartz penetration probes with 3.7 mm diameters were used as parallel plates. Measurements were performed with different heating rates and isothermally with samples of different initial height. In these experiments, the sample completely filled the area between the plates in a helium flushed atmosphere.

Samples cut from cast rods do not have a perfectly smooth finish, and the force applied by the plates at low temperatures will not be uniformly

distributed on the sample. Once the temperature is high enough and the viscosity low enough, material will flow and completely fill all the volume as well as the microcracks between the plates and the sample. Thus, a two-step process is required to measure viscosity using parallel plate. First, the sample is heated to a temperature of 683 K, where the material is fluid enough to fill the volume completely using small forces (2.6 N). Then the sample is cooled to 473 K at a rate of 200 K per minute. Now that the sample is firmly seated between the plates, a constant heating rate is applied and the viscosity is measured.

Fig. 3.1 shows the viscosity as measured with a heating rate of 0.833 K/s, a force of 2.6 N, and an initial height of 0.3 mm. The measured viscosity decreases with increasing temperature from 2.0×10^8 poise at 685 K to 6.0×10^6 poise at 743 K. Here, the supercooled liquid finally starts to crystallize, resulting in a sudden stiffening of the sample. For temperatures smaller than 695 K, the measured viscosities are higher than the equilibrium viscosities. Here, the alloy is still in the glass transition region for the respective heating rate, as separate DSC investigations (see Fig. 1, Chapter 1) reveal. In this region, lower heating rates or isothermal measurements have to be used to obtain the equilibrium viscosity of the supercooled liquid. Large heating rates shift the crystallization to higher temperatures (e.g., up to 763 K at a rate of 1.167 K/s). Thus, the low viscosity range down to 10^6 poise can be measured as well using large heating rates.

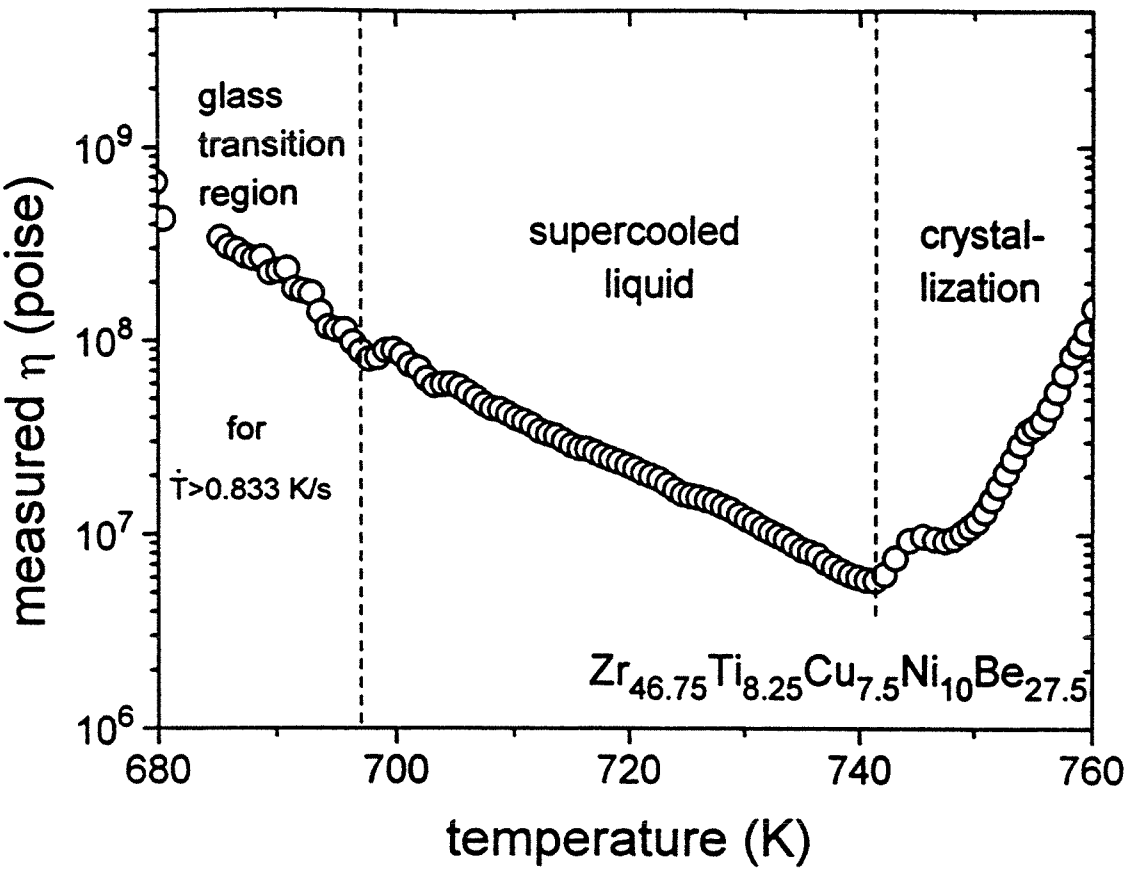

Fig. 3.1. Parallel plate measurement of the viscosity as a function of temperature of the $Zr_{46.75}Ti_{8.25}Cu_{7.5}Ni_{10}Be_{27.5}$ alloy for a heating rate of 0.833 K/s.

The measured value of the viscosity depends on the aspect ratio between the sample height, h, and the radius of the probe, a, since Eq. 2.14 was derived by neglecting the velocity normal to the plates. Applying results obtained by Gent [1], the measured viscosity fits a parabolic function:

$$\eta = b + cx^2 \tag{3.1}$$

were x is the aspect ratio (h/a), and b and c are fitting parameters. This was verified experimentally with isothermal measurements performed using silicone at ambient temperature. The low viscosity of silicone at room temperature allows large variation in the aspect ratio from 1 to less than 0.07. Fig. 3.2 shows the measured viscosity as a function of the aspect ratio for silicone. The measured viscosity is best fitted by a parabolic fit, Eq. 3.1.

The measured viscosity of $Zr_{46.75}Ti_{8.25}Cu_{7.5}Ni_{10}Be_{27.5}$ as a function of aspect ratio at a temperature of 703 K is shown in Fig. 3.3. Viscosity for different heating rates as well as isothermal measurements were fitted to Eq. 3.1. The value of viscosity obtained by extrapolating the aspect ratio to zero was taken as the real equilibrium viscosity value. This plot reveals that the measured viscosity does not change with heating rate. For this temperature, the relaxation time to obtain an equilibrium viscosity is smaller than the experimental times for these heating rates. The measured values of viscosity obtained for aspect ratios smaller than 0.25 correspond to these equilibrium viscosity values within the experimental error.

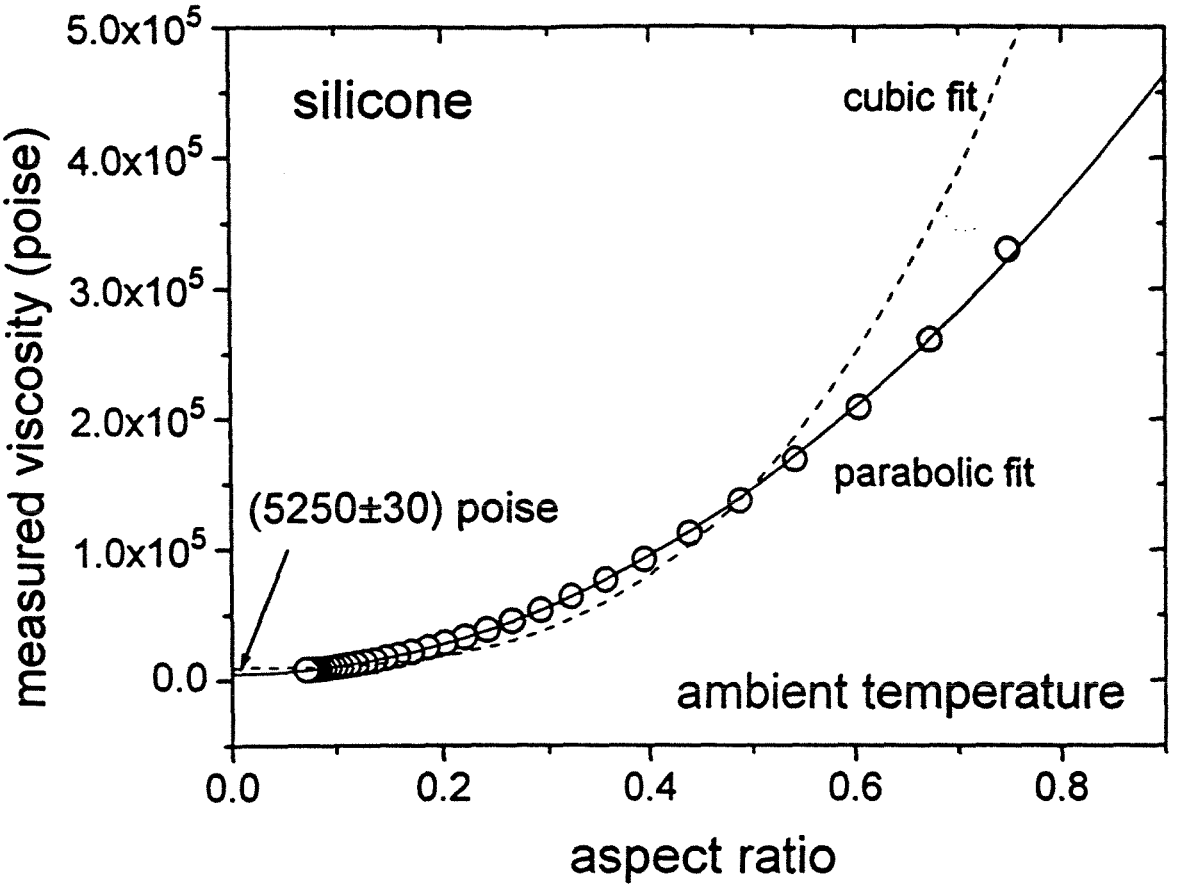

Fig. 3.2. Measured viscosity of silicone at room temperature showing the dependence of viscosity with aspect ratio using parallel plate rheometry.

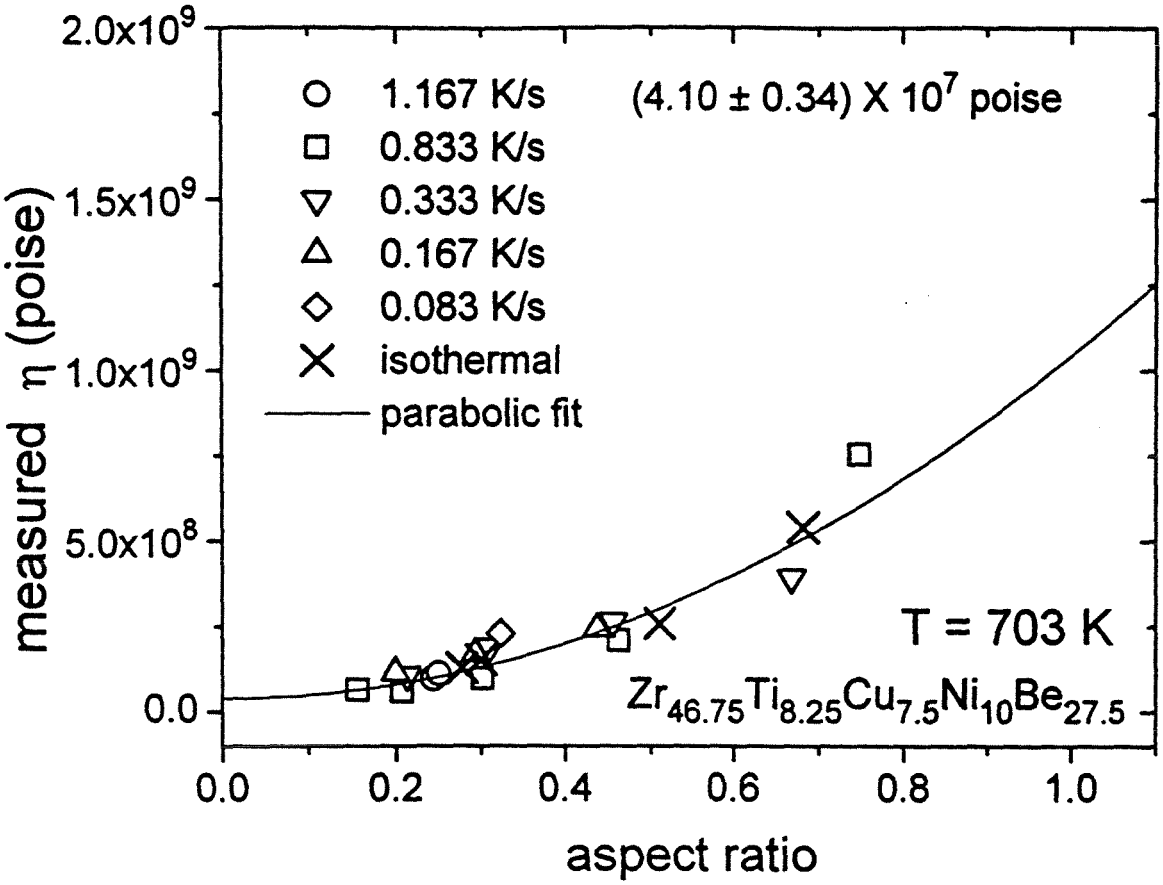

Fig. 3.3. Measured viscosity of the $Zr_{46.75}Ti_{8.25}Cu_{7.5}Ni_{10}Be_{27.5}$ alloy as a function of aspect ratio at 703 K.

The viscosity of the metastable supercooled liquid as a function of temperature as extracted from the measurements with different heating rates and isothermally for parallel plate rheometry is shown in Fig. 3.4 as an Arrhenius plot. The viscosity data cover about 30% of the entire supercooled liquid region of this alloy between the glass transition region (for a heating rate smaller than 0.0167 K/s) and the melting point T_{liq} = 1050 K. The data were fitted by the Vogel-Fulcher relation from Chapter 1:

$$\ln \eta = A + B/T\text{-}T_o \qquad (1.4)$$

where A, B, and T_o are fitting parameters. The best fit to the viscosity data was found for T_o = 352 K. We find that A = (-9.0 ± 2.0) and B = (9.442 ± 1.64) x 10^3 K. With this small Vogel-Fulcher temperature, T_o, relative to the glass transition temperature, a Vogel-Fulcher relationship yields a reasonable viscosity of 70 poise at the liquidus temperature, a value which was separately verified by capillary flow measurements (see later section).

In order to measure the viscosity from 10^{14} to 10^9 poise, three-point bending was used. A typical three-point bending measurement is shown in Fig. 3.5. A beam of rectangular cross section of 0.722 mm by 0.353 mm, a force of 0.05 N, and a heating rate of 0.833 K/s was used. The measured viscosity decreases with increasing temperature. The rise in viscosity at a temperature of 670 K is the position at which the beam has hit the bottom limit of the three-point apparatus (about 1 mm of deflection), and is not a

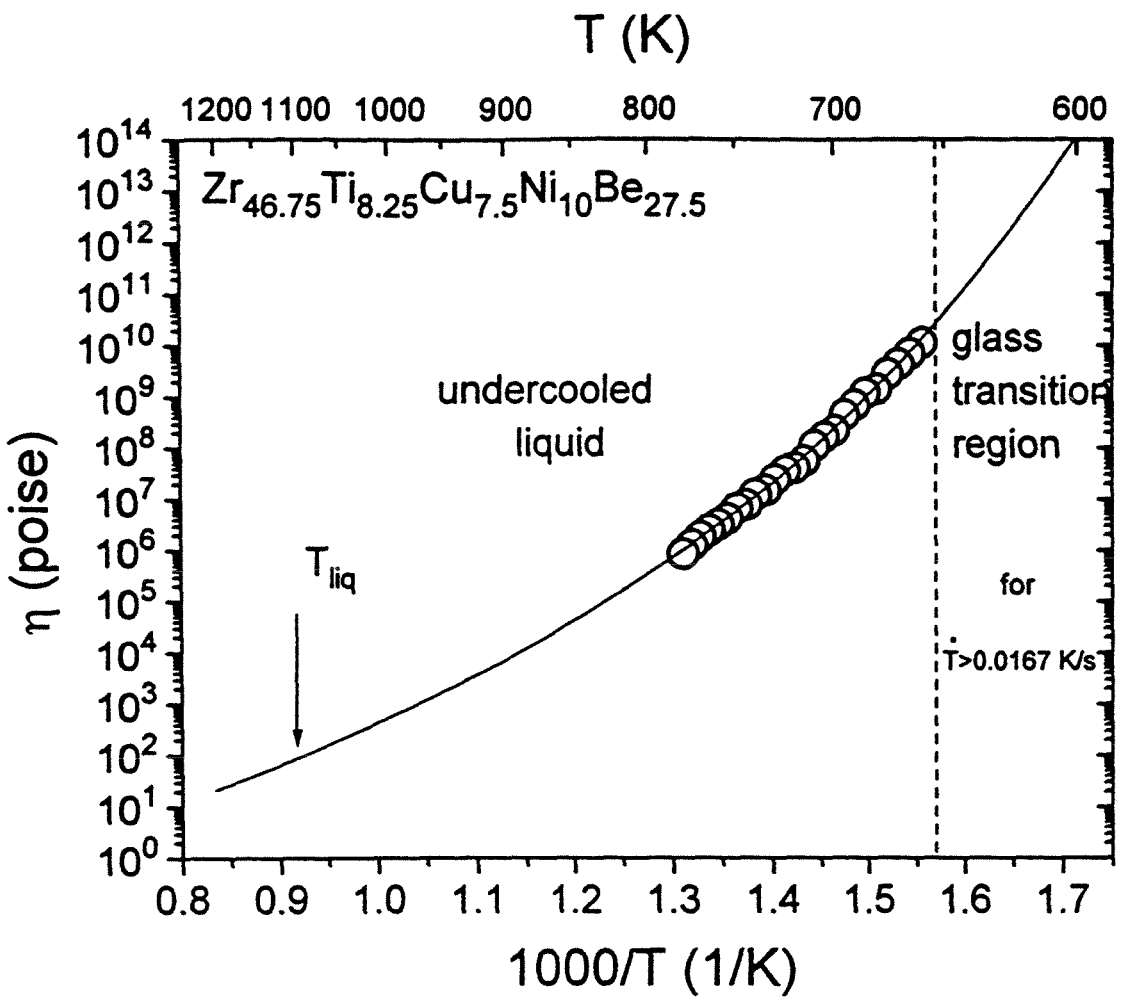

Fig. 3.4. Equilibrium viscosity as a function of temperature for the undercooled liquid as measured using parallel plate rheometry with different heating rates as well as isothermally.

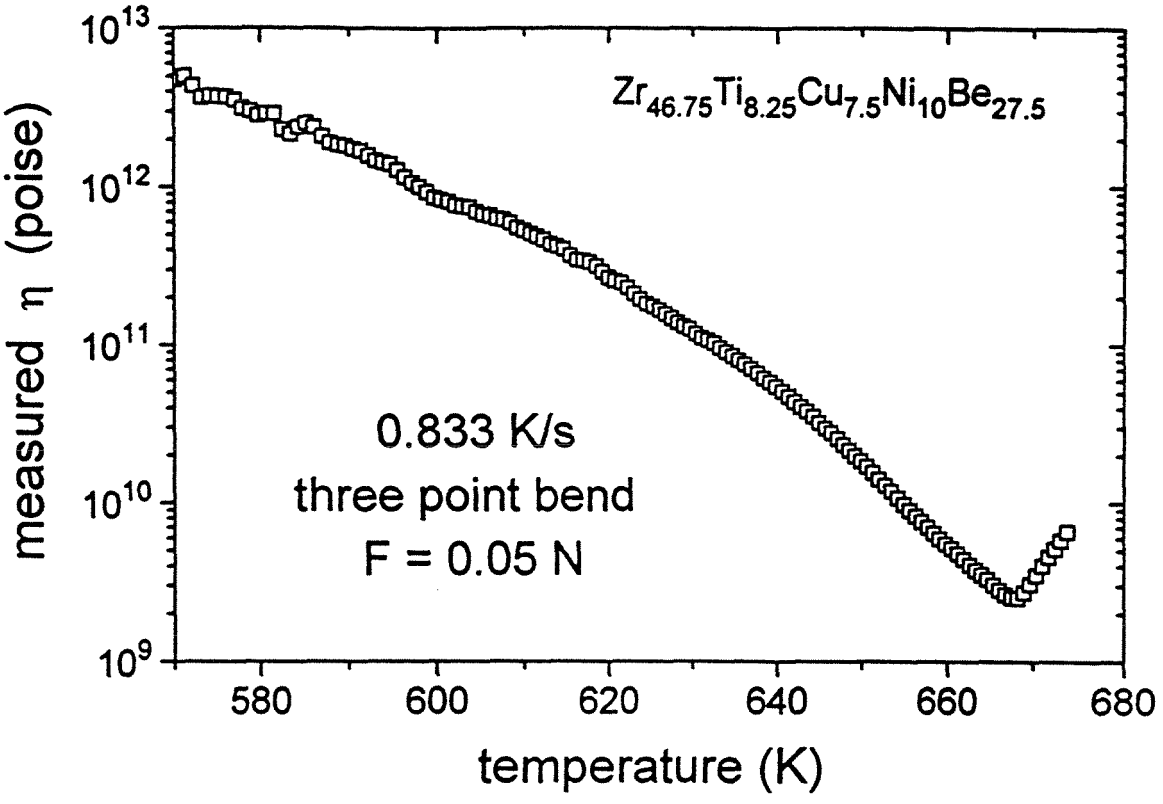

Fig. 3.5. Three-point bending measurement of the viscosity as a function of temperature of the $Zr_{46.75}Ti_{8.25}Cu_{7.5}Ni_{10}Be_{27.5}$ alloy for a heating rate of 0.833 K/s.

real viscosity effect. The measured viscosity is found to be independent of force and beam cross section, provided the height of the beam is less than 1/5 of the span of the support knife edges. Fig. 3.6 shows two measurements with different heating rates. The samples for these measurements were cut from the same cast rod, and therefore had the same thermal history. As discussed above, relaxation effects are different for the two different heating rates. This is clearly seen in that the viscosity of the metallic glass in the glassy region for the smaller heating rate more closely approaches the equilibrium value of viscosity as defined by the Vogel-Fulcher relation. Once the viscosity is below 10^{11} poise, the relaxation time is smaller than ten seconds, and the viscosity of the two measurements become similar.

In order to measure equilibrium viscosities of 10^{10} poise and higher, and avoid relaxation effects, isothermal measurements (from 583 K to 653 K in 5 K increments) using three-point bending were also performed [2]. Fig. 3.7 shows an isothermal measurement at a temperature of 583 K. Upon heating the amorphous sample to the measurement temperature, the measured viscosity relaxes to the equilibrium value. Once the temperature is reached, the relaxation can be fit to a Kohlrausch-Williams-Watts "stretched exponential relaxation" (see for example ref. [3] or [4]) growth, with mean relaxation time τ:

$$\eta(t) = \eta_{eq}\left(1 - e^{-(t/\tau)^{\beta}}\right) \tag{3.2}$$

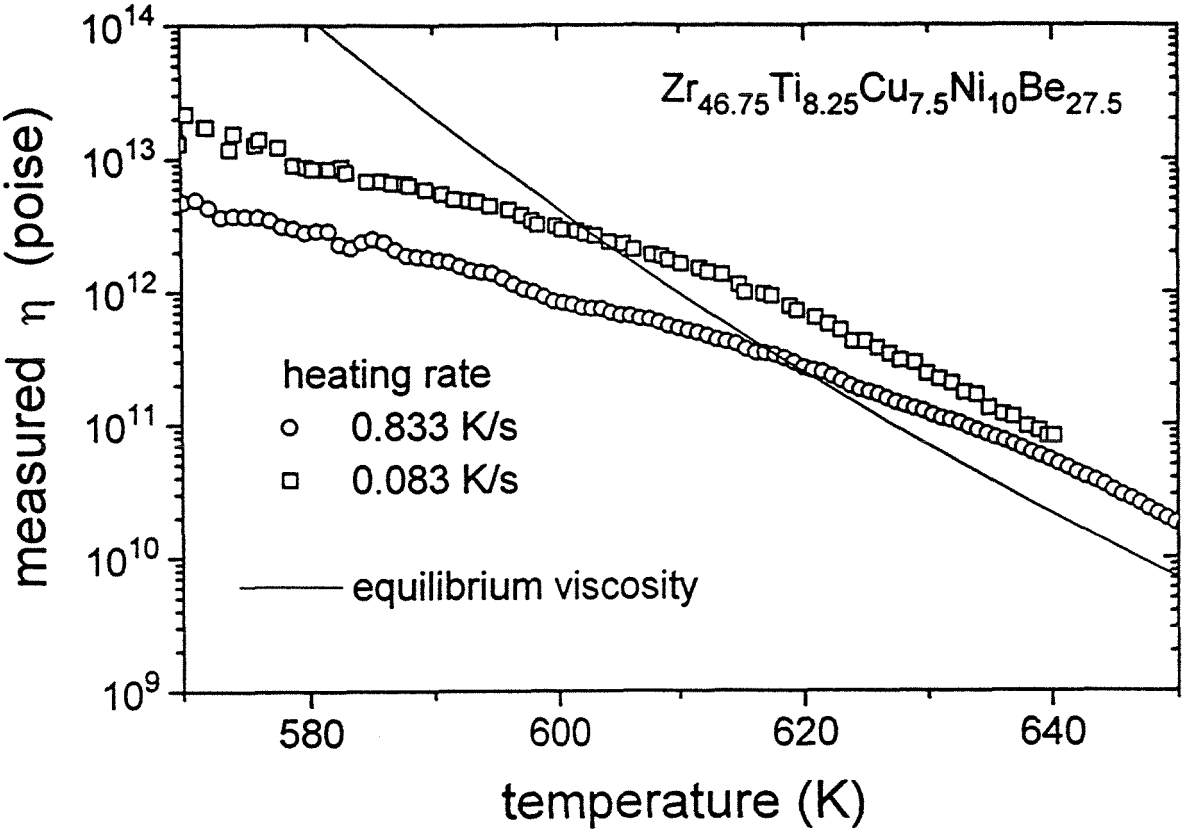

Fig. 3.6. Comparison of two measurements of viscosity with different heating rates using three-point bending showing the different relaxation effects.

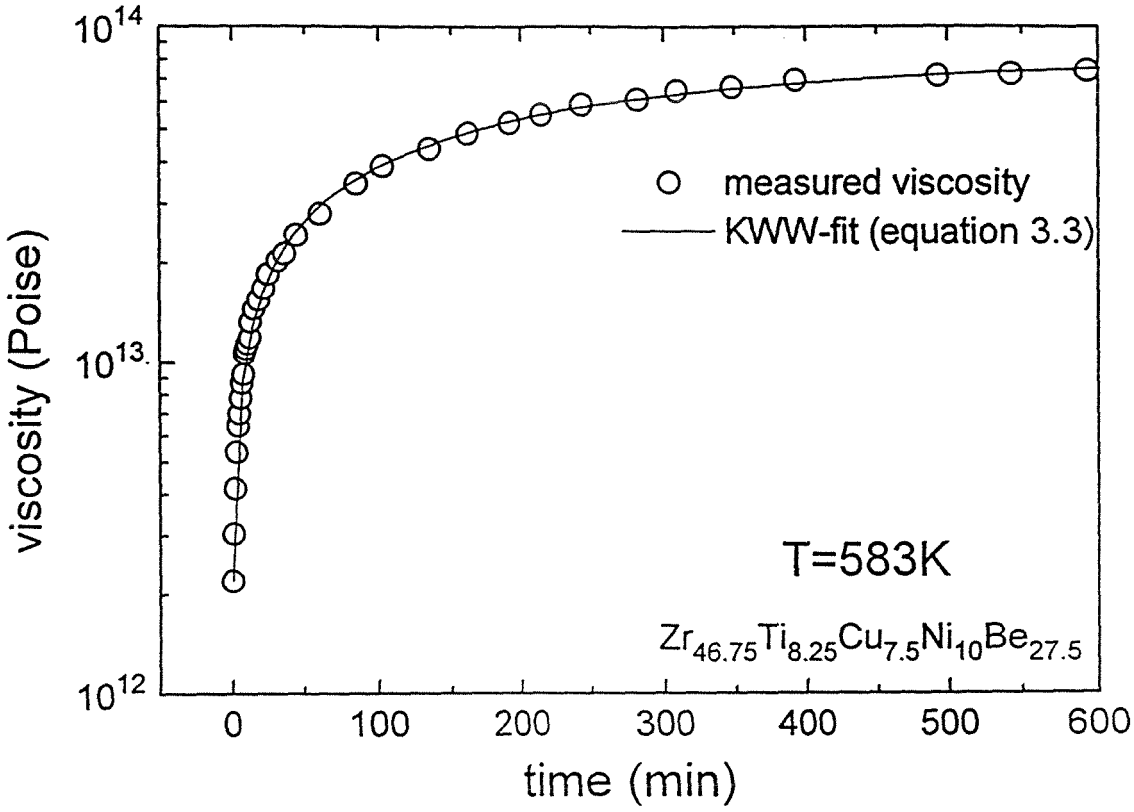

Fig.3.7. Isothermal measurement of viscosity of the $Zr_{46.75}Ti_{8.25}Cu_{7.5}Ni_{10}Be_{27.5}$ alloy using three-point bending at a temperature of 583 K.

where β, τ and η_{eq} are fitting parameters. At this temperature, the best fit to the viscosity data yield η_{eq} = 8.42 (± 1.6) X 10^{13} poise, β = 0.74 ± 0.01, and τ = 12420 ± 660 seconds. The value of β is typical for strong glasses like oxides (around 0.7), whereas for conventional metallic glasses, values of β are found to be nearer 0.4 [5]. In fact, we will see in Chapter 4, that this β is consistent with strong glass behavior, and bulk metallic glass behaves more like strong glass.

The mean relaxation times as measured by isothermal viscosity measurements for different temperatures scale with the viscosity itself according to:

$$\eta(poise) = 7 \times 10^{9} \times \tau(\text{sec}) \tag{3.4}$$

This can be related to the high frequency shear modulus:

$$\eta = G_{\infty}\tau \tag{3.5}$$

according to arguments given in ref. [6].

As was shown in Fig. 1.1, the specific heat capacity data measurements have an onset and completion temperature. With a constant heating rate, the total time for the sample to relax from the glass to the supercooled liquid can be measured, i.e., the time to undergo the glass transition. This 'total relaxation time' can be plotted as a function of the average temperature through the glass transition, as shown in Fig. 3.8. Because these were not isothermal measurements, there were a distribution of relaxation times through the glass transition. The values as shown in

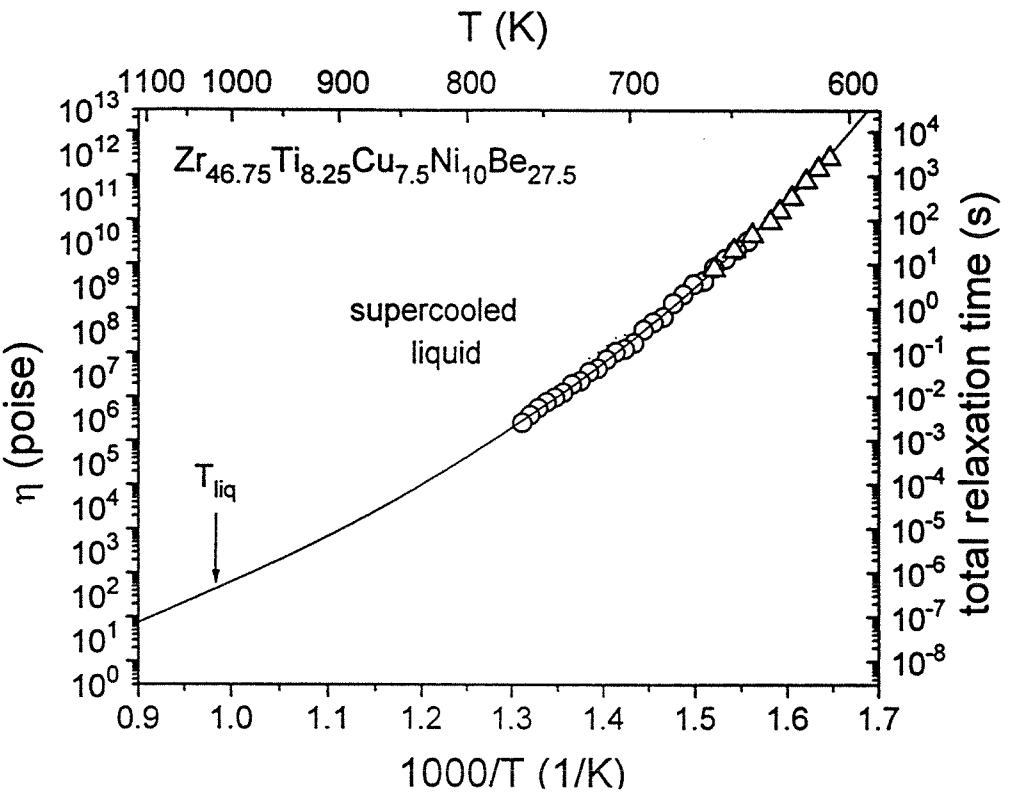

Fig. 3.8. The total relaxation time (triangles) as measured by specific heat capacity as compared to the measured viscosity (circles) of the $Zr_{46.75}Ti_{8.25}Cu_{7.5}Ni_{10}Be_{27.5}$ alloy.

Fig. 3.8 are a factor of 5 times larger than the relaxation times as measured isothermally with viscosity. Also shown in Fig. 3.8 is the equilibrium viscosity as measured by parallel plate. The total relaxation time through the glass transition fit the Vogel-Fulcher relation as measured by viscosity. By measuring the isothermal viscosity, the relaxation time can be directly extracted. Measurements that require a constant heating rate, like specific heat capacity, make relaxation phenomena more difficult to interpret.

Parallel plate rheometry and beam-bending both can measure viscosity in the region from 10^8 to 10^9 poise. The measured viscosity for beam-bending at its high temperature extreme coincides with the measured viscosity for parallel plate rheometry at its low temperature extreme. Because the two methods involve different geometries for application of force and measurement of the resulting flow, the accuracy of the viscosity measured by each can be verified. Within the experimental precision of our measurements, the viscosity measured by both methods are in agreement as shown in Fig. 3.9.

The measured viscosity in the glass transition region depends on the heating rate. As the glass is heated above the glass transition into the supercooled liquid region, the measured viscosity is no longer heating rate dependent, also shown in Fig. 3.9, for parallel plate measurements. In the glass transition region and below, the experimental time scales are shorter than the relaxation time of the glass, and the measured viscosity is heating rate dependent. Thus, beam-bending viscosities shown in Fig. 3.9 (and Fig.

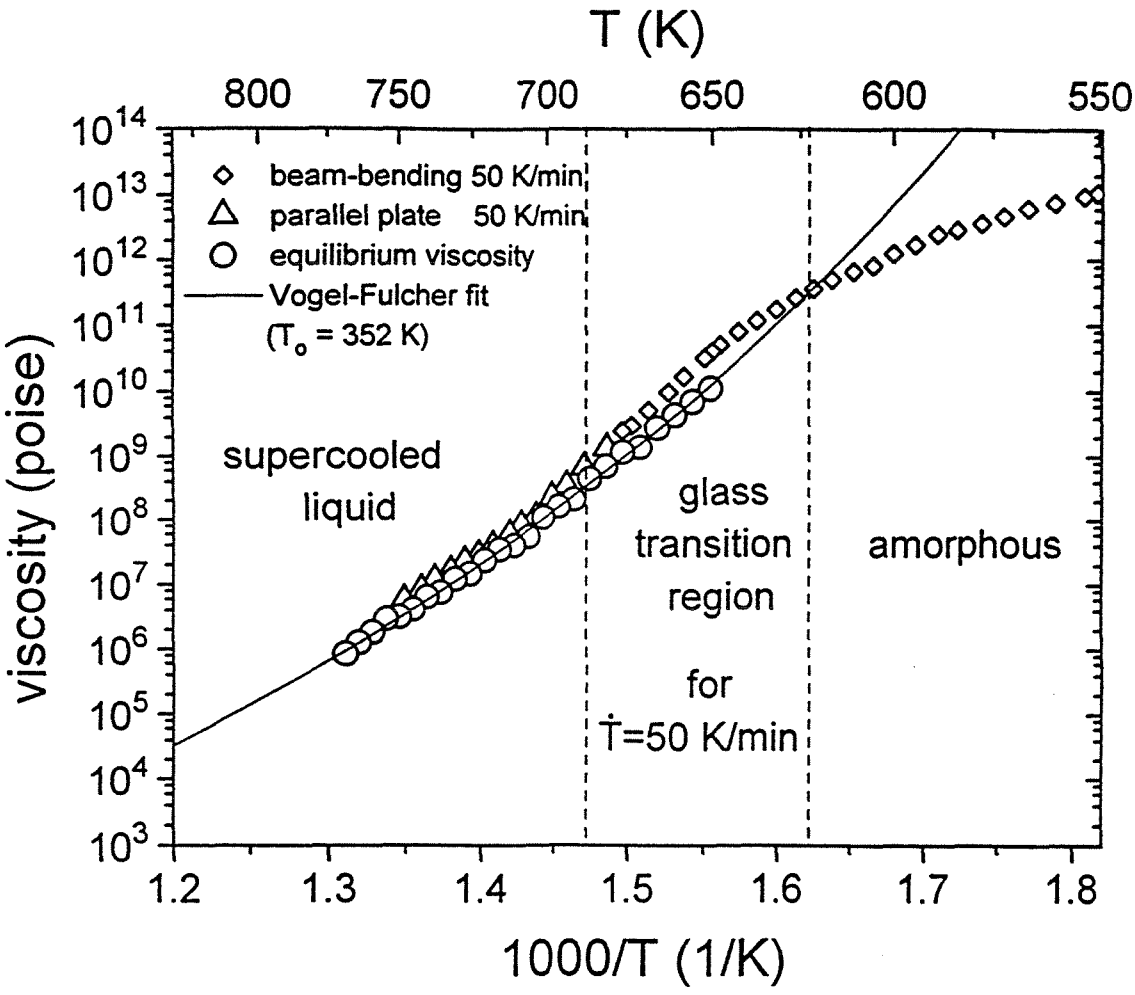

Fig. 3.9. Viscosity as measured for beam bending and parallel plate rheometry for a heating rate of 0.833 K/s compared to the equilibrium viscosity.

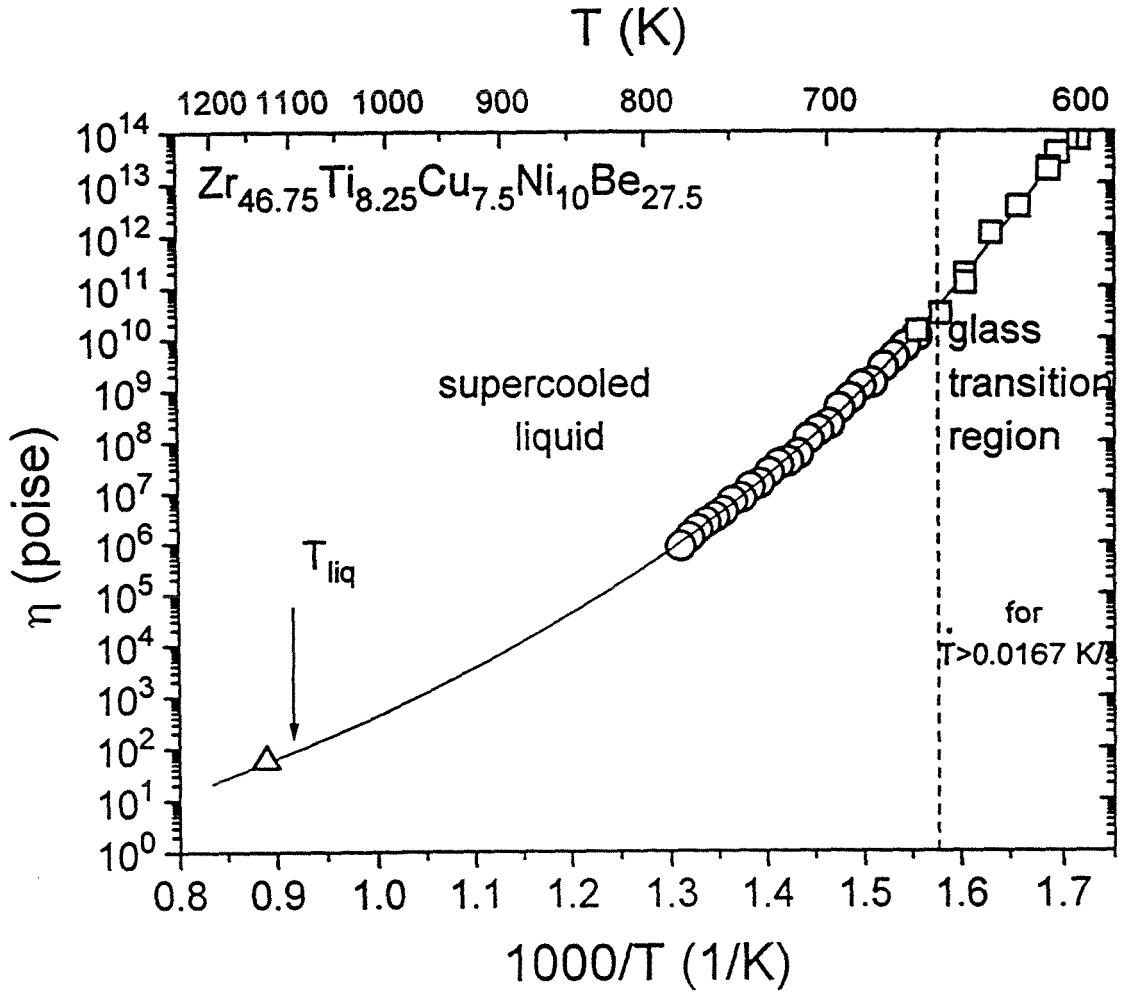

Fig. 3.10. Equilibrium viscosity as a function of temperature for the undercooled liquid of the $Zr_{46.75}Ti_{8.25}Cu_{7.5}Ni_{10}Be_{27.5}$ alloy as measured using parallel plate rheometry (circles), three-point bending (squares) and capillary flow (triangle).

3.6) are not equilibrium viscosities since they lie in the glass transition region. In this region, the measured viscosity will be higher than the equilibrium value. In the amorphous state, they are lower than the equilibrium value [7]. As the glass relaxes towards equilibrium, the viscosity increases in the amorphous state to an equilibrium value (see also Fig. 3.7).

As previously mentioned, upon extrapolating the Vogel-Fulcher fit for the $Zr_{46.75}Ti_{8.25}Cu_{7.5}Ni_{10}Be_{27.5}$ alloy to the liquidus temperature, T_{liq}, a viscosity of about 70 poise is found. Experimental data of capillary flow measurements provided by A. Masuhr are shown in Fig. 3.10 at temperature T_{liq} + 50 K, as well as isothermal three-point bending viscosity measurements. As can be seen, all viscosity data follow the Vogel-Fulcher relation fit to the parallel plate data. Although there is no data for the region between 10^6 and 10^2 poise, the fact that equilibrium viscosity measurements from completely different geometries of flow fall on the same functional relation indicate that the viscosity curve is well defined and varies continuously with temperature. As far as the author is aware, this study includes the largest range of viscosity ever measured for a glass forming metallic liquid alloy as of this date.

References

[1] A. N. Gent, Brit. Jour. Appl. Phys. **11**, 85 (1960).

[2] R. Busch, E. Bakke, and W. L. Johnson, (unpublished research).

[3] C. A. Angell, Science **267**, 1924 (1995).

[4] F. H. Stillinger, Science **267**, 1935 (1995).

[5] T. Komatsu, K. Fujita, K. Matusita, K. Nakajima, and S. Okamoto, J. Appl. Phys. **68**, 2091 (1990).

[6] C. A. Angell, P. H. Poole, and J. Shaw, Il Nuovo Cimento **16**, 993 (1994).

[7] C. A. Volkert and F. Spaepen, Acta metall. **37**, 1355 (1989).

Chapter 4:

STRONG GLASS BEHAVIOR OF BULK METALLIC GLASS

As discussed in the Introduction, the viscosity of a material plays a key role in determining the nucleation of the crystalline state from the liquid. However, the role of viscosity in glass forming ability depends also on the material itself. Glasses are made from numerous systems, including such materials as oxides and polymers, for example. Since each of these systems have different networking and bonding between its constituent atoms, viscosity alone does not determine glass forming ability. But when viscosities between metallic glasses are compared, the viscosity dependence with temperature can be used as an indicator of the glass forming ability.

In order to compare the various glasses to one another, a system by Angell [1] was developed. Since the different glasses have different values of T_g, the viscosity cannot be simply plotted as a function of temperature. A better interpretation is found by plotting the log of the viscosity as a function of T_g/T, an Arrhenius plot with inverse temperature reduced by the glass transition temperature, as in Fig. 4.1. Plotted are the viscosity of six glasses, including the bulk metallic glass, $Zr_{46.75}Ti_{8.25}Cu_{7.5}Ni_{10}Be_{27.5}$, as a function of temperature. The silicate and the polymer glass (o-terphenyl) exhibit the two extremes in viscous behavior with temperature, called strong and fragile liquid behavior respectively. Again, this does not

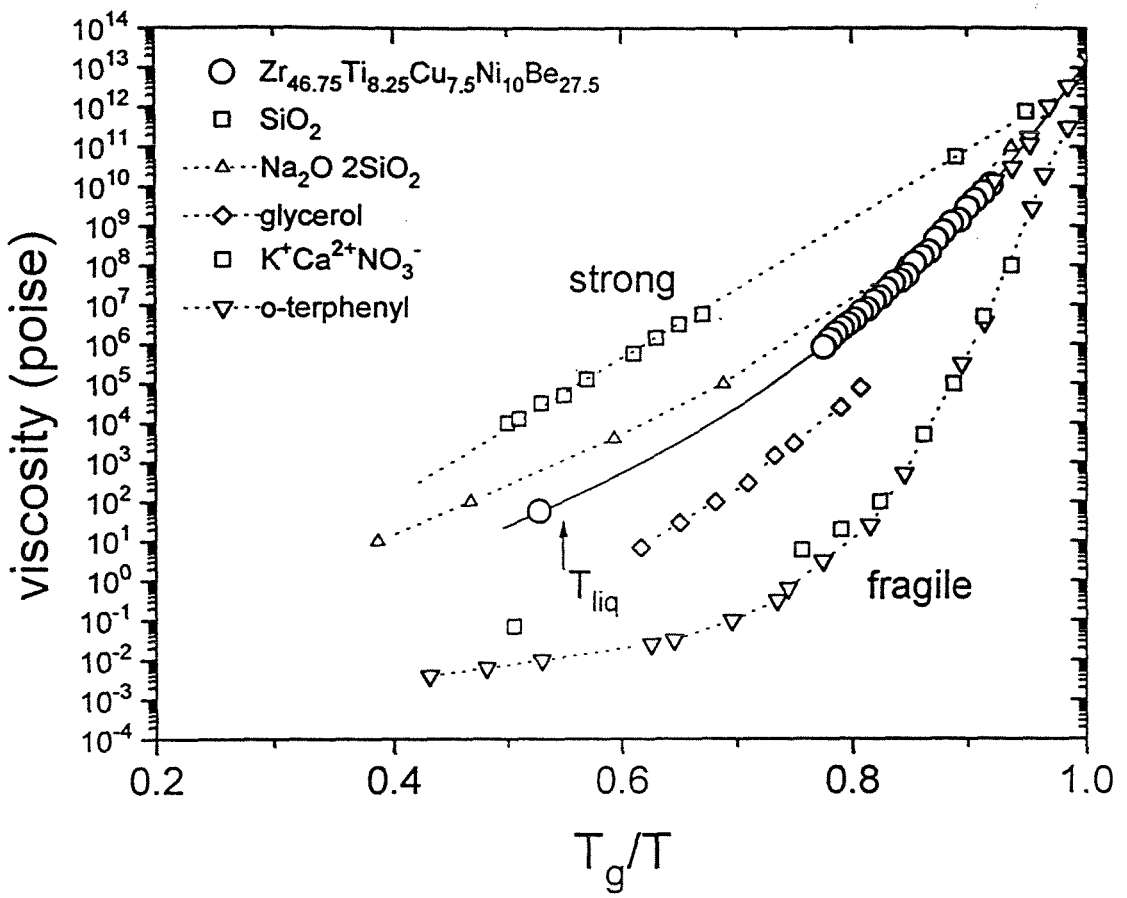

Fig. 4.1. Angell plot of several glass forming systems showing the regions of strong and fragile glass behavior.

imply one as a better glass former than the other, but rather indicates the relative sensitivity of the liquid structure to changes in temperature.

The strong glass behavior of silica exhibits a large viscosity at the melting point of order one thousand poise. For the $Zr_{46.75}Ti_{8.25}Cu_{7.5}Ni_{10}Be_{27.5}$ alloy, extrapolating the equilibrium curve to the liquidus temperature, T_{liq}, a viscosity of about 70 poise is found, which agrees well with the viscosity as measured by capillary flow (see Fig. 3.10). This value is smaller than for the silicate glasses because the slope of the viscosity curve and the Vogel-Fulcher temperature, T_o, is larger for this bulk metallic glass former compared to silicates (see Fig. 4.1). The melting point viscosity is of the same order as the measured melting point viscosities of some multicomponent metallic melts, such as 69.3 and 61.5 poise for $Pd_{77.5}Si_{16.5}Cu_6$ [2] and $Pd_{82}Si_{18}$ [3], respectively. The measurement of viscosity of the equilibrium melt and near the liquidus of the $Zr_{46.75}Ti_{8.25}Cu_{7.5}Ni_{10}Be_{27.5}$ alloy as a function of temperature will be subject to further investigation outside of this study [4].

The original Vogel-Fulcher relation, eq. 1.4, can be modified using one parameter, *D*, the fragility index, to reproduce the patterns found in Fig. 4.1. Equation 1.4 is then rewritten as:

$$\ln \eta = A + {}^{DT_o}\!/_{T - T_o} \tag{4.1}$$

Arrhenius behavior is in the limit where $D \to \infty$ or $T_o \to 0$. The fragility index, D, determines how closely the system's viscosity approaches the Arrhenius law. Arrhenius behavior or a Vogel-Fulcher relationship with a small T_o is found for strong glasses, like silicates, and D is of order 100. For fragile glasses, like some polymers, a T_o value closer to T_g is found and D can be as low as 2 [5]. In this same region, our alloy shows a viscosity temperature dependence that is more consistent with strong glass materials, as shown in Fig. 4.1, with T_o = 352 K and D = 19.8.

The viscosity for different systems of metallic glasses, along with the strong silicate glass, are shown in Fig. 4.2 [6]. Data for viscosity below 10^{10} poise for metallic glasses, except for the $Zr_{46.75}Ti_{8.25}Cu_{7.5}Ni_{10}Be_{27.5}$ alloy, was not previously available due to the onset of crystallization, which halted further measurement into the supercooled liquid. From this plot, an important factor in glass forming ability can be deduced. The critical cooling rate for glass formation can be correlated inversely to the fragility index. The stronger the glass (larger D), the smaller the critical cooling rate. The $Zr_{46.75}Ti_{8.25}Cu_{7.5}Ni_{10}Be_{27.5}$ alloy has a fragility index of 19.8 and a critical cooling rate of 10 K/s and forms a bulk metallic glass (12 m m thick), whereas $Au_{77.8}Ge_{13.8}Si_{8.4}$ has D = 8.4 and $R_c = 10^6$ K/s and can only be made in thin strips (< hundred microns). Since these metallic glass systems have similar structures and bonding mechanisms between their constituent atoms, direct comparisons can be made of the viscosity behavior to determine their respective glass forming ability. According to

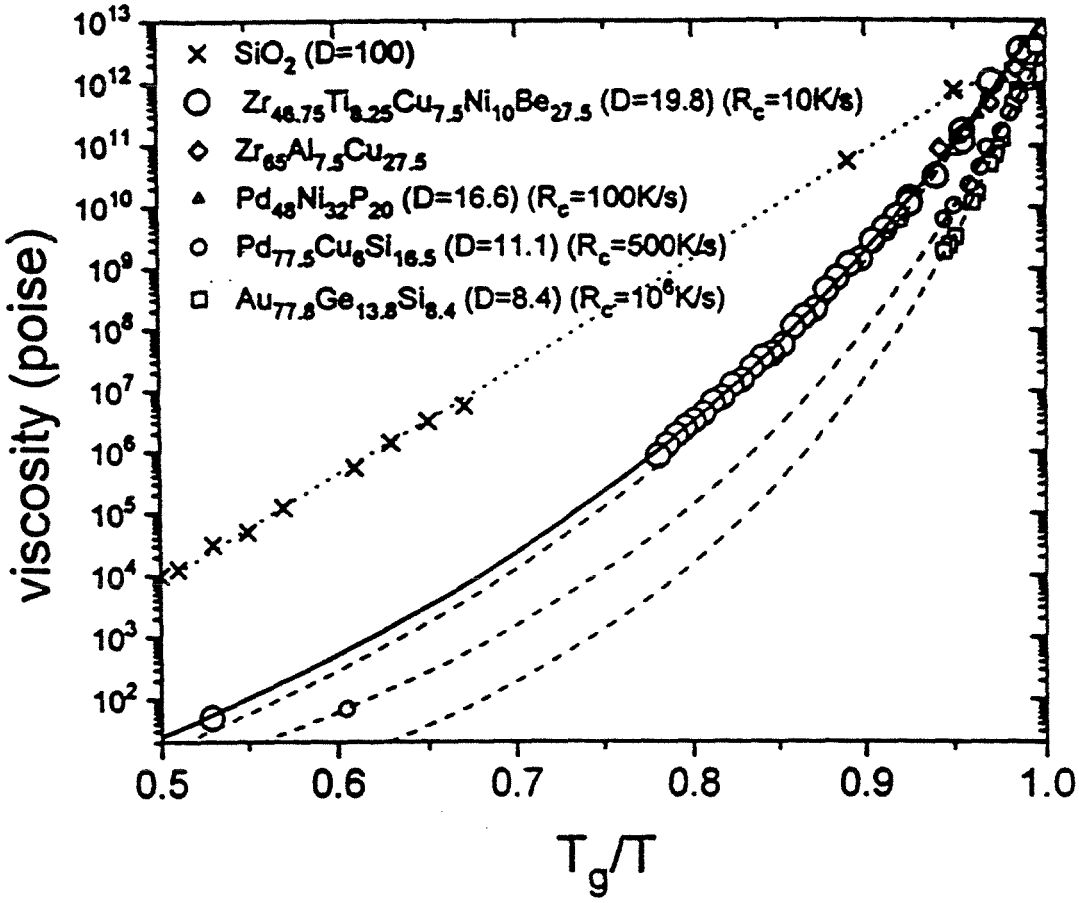

Fig. 4.2. Angell plot of metallic glasses compared to a silicate glass with critical cooling rates and fragility index.

eq. 1.1, the nucleation rate is proportional to $1/\eta(T)$. As seen in figure 4.2, $1/\eta(T)$ is orders of magnitude higher for strong glasses in the region below the melting point to T_g. The kinetic contribution to the nucleation rate scales with the inverse of the fragility index, where metallic glasses with higher index having stronger glass forming ability.

As discussed in Chapter 3, the relaxation of the isothermal viscosity measurements can be fit with eq. 3.3. The strong/fragile behavior of glass can also be seen in the kinetic aspect of the relaxation to the equilibrium configuration in the supercooled liquid. From the fit to the viscosity data with eq. 3.3, β is found to be 0.74 for our bulk metallic glass. This is consistent with strong glass behavior like oxides, where β is around 0.7. Values of β for other metallic glasses is around 0.4 (see ref. 5, Chapter 3). β represents the width of the distribution of relaxation times and $0 < \beta \leq 1$. The viscous behavior below the melting point and the relaxation in the supercooled liquid can be used to measure the glass forming ability.

The other factor playing a role in crystal nucleation as discussed in the Introduction was the Gibbs free energy between the liquid and the crystal. As investigated by Busch et al. [6], the glass formers with the lowest critical cooling rates have smaller Gibbs free energy differences than the glass formers with high critical cooling rates (see Fig. 4.3). This means that the driving force for crystallization decreases with increasing glass forming ability. This effect mainly originates from the fact that bulk metallic glasses

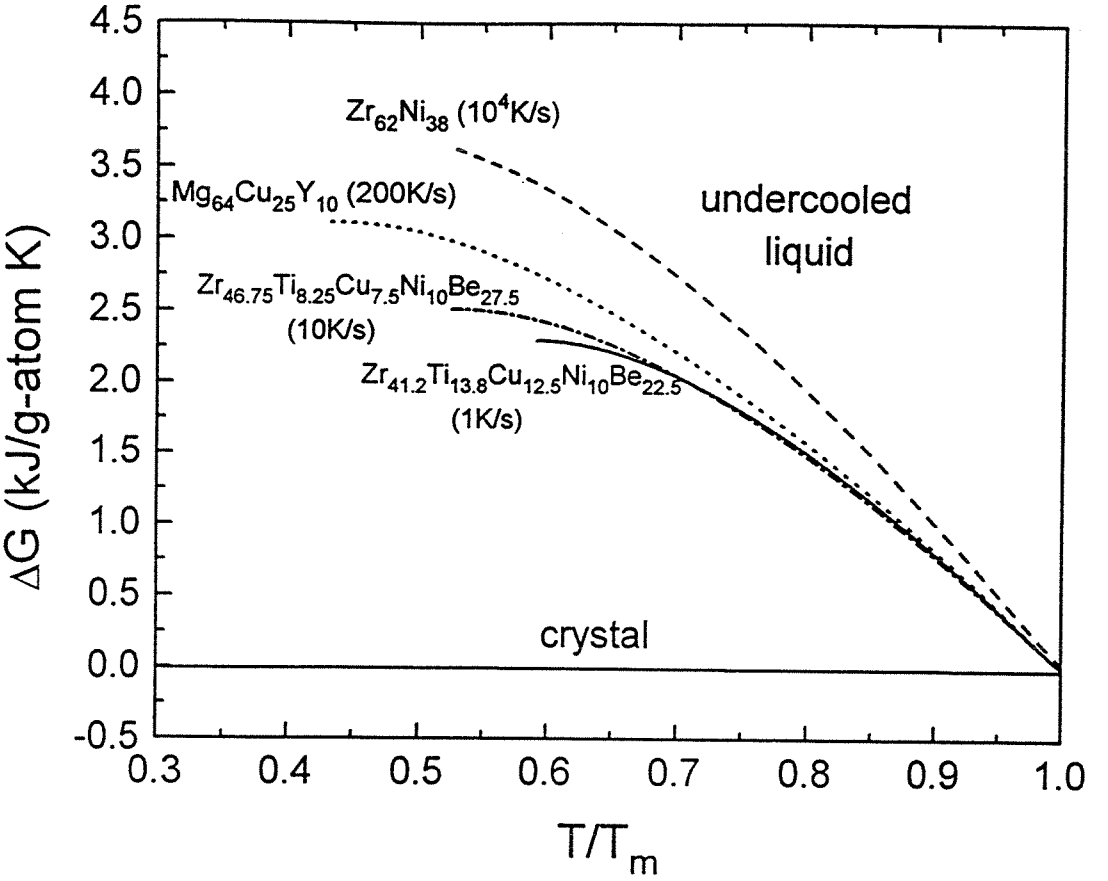

Fig. 4.3. Gibbs free energy difference between the undercooled liquid and the crystalline mixture for different metallic glass forming alloys. Reproduced from ref. 6.

are found to have small entropies of fusion which determine the slope of the differential free energy curve for the crystal/liquid transition at the melting point. The small entropy at the melting point implies that the bulk glass formers have small free volume [7] and tend to short range order [8]. The higher viscosity from the melt to the glass transition temperature and the smaller Gibbs free energy difference compared to the crystal both favor bulk glass formation.

As mentioned earlier, the Angell plot can provide a general picture of the sensitivity of the liquid structure to changes in temperature. Certain types of liquids are found in the two extremes of strong and fragile behavior. The structure of oxide glasses, like silicate, can be described by a continuous random network [9] and exhibit strong glass behavior. Some polymers, at the other extreme of fragile glass behavior, have structures best described by van der Waals interactions with many π bonds [1]. The most satisfactory model for metallic glass structure has been the dense random close-packing model [10,11]. As can be seen in Fig. 4.2, the bulk metallic glass has viscous behavior more consistent with strong glass behavior, although its structure cannot be described by an open network of covalent bonds. The higher viscosity for bulk metallic glass is consistent with the free volume theory of glasses [7], as discussed above.

In the free volume theory, the Doolittle equation can be used to

connect the viscosity with the total free volume, V_f:

$$\eta = A\exp(B/V_f) \tag{4.2}$$

where A and B are constants related to the minimum amount of free volume needed for molecular transport. The total free volume, V_f, can be approximated by:

$$V_f \approx \alpha(T - T_0) \tag{4.3}$$

where α is the thermal expansion coefficient in the vicinity of the glass transition and T_o is the temperature at which the free volume tends to zero. Combining eqs. 4.2 and 4.3, one obtains the Vogel-Fulcher relation, eq. 1.4:

$$\ln \eta = A' + B'/T\text{-}T_o \tag{1.4}$$

An alternative model was established by Adams and Gibbs [13] in which the configurational entropy is the parameter to describe viscous flow as a function of temperature. The viscosity can be written as:

$$\eta = A\exp\left(C/TS_c\right) \tag{4.4}$$

where A and C are constants and S_c is the configurational entropy. Eq. 4.4 can be rewritten as:

$$\eta = A'\exp\left(C'/\ln(T/T_0)\right) \tag{4.5}$$

or:

$$\eta = A'' \exp\left(C''/T - T_0 \right) \tag{1.4}$$

depending on the functional form for the excess heat capacity in evaluating the configurational entropy. ΔC_p = a constant yields eq. 4.5, whereas ΔC_p = K/T yields eq. 1.4, the Vogel-Fulcher relation. The model which best describes the viscosity dependence with temperature of our bulk metallic glasses has yet to be determined.

References

[1] C. A. Angell, Science **267**, 1924 (1995).

[2] J. Steinberg, S. Tyagi, and A. E. Lord, Jr., Appl. Phys. Lett. **38**, 878 (1981).

[3] J. Steinberg, S. Tyagi, and A. E. Lord, Jr., Acta metall. **29**, 1309 (1981).

[4] A. Masuhr, R. Busch, E. Bakke, and W. L. Johnson, (unpublished research).

[5] D. J. Plazek and K. L. Ngai, Macromolecules **24**, 1222 (1991).

[6] R. Busch, E. Bakke, and W. L. Johnson, Mat. Sci. Rev. (1996, in press).

[7] D. Turnbull and M. H. Cohen, J. Chem. Phys. **52**, 3038 (1970).

[8] R. Busch, S. Schneider, A. Peker, and W. L. Johnson, Appl. Phys. Lett. **67**, 1544 (1995).

[9] W. H. Zachariasen, J. Am. Chem. Soc. **54**, 3841 (1932).

[10] M. H. Cohen and D. Turnbull, Nature **203**, 964 (1964).

[11] G. S. Cargill, Solid State Phys. **30**, 227 (1975).

[12] P. Ramachandrarao, B. Cantor, and R. W. Cahn, J. Mat. Sci. **12**, 2488 (1977).

[13] G. Adam and J. H. Gibbs, J. Chem. Phys. **43**, 139 (1965).

Chapter 5:

PROCESSING BULK METALLIC GLASS

Because of the thermal stability of bulk metallic glass alloys in the undercooled liquid region, which results in a large temperature region above the glass transition temperature before the onset of crystallization, the temperature of the glass can be raised to values where the viscosity is as low as 10^6 poise. At these low values of viscosity, shaping and forming operations can be done with forces of the order of 1 atmosphere, similar to glass blowing of oxide glasses. This type of metal processing is novel in that crystalline metals melt long before softening to this point. Melting is a discontinuous phase change whereby viscosity jumps from a solid-like to a fluid-like value. Since the temperature at which the glass starts to soften is near T_g, processing can be done at 2/3 of the melting temperature. By processing a viscous liquid, one increases die lifetime, broadens the available die materials that can be used, reduces risk of oxidation and reduces solidification shrinkage associated with the liquid/crystal phase transformation.

Once the viscosity of a material has been measured, the relationship between stress and strain rate are known. All the viscosity measurements in this study were made for small strain rates (less than 10^{-1} /s). Fig. 5.1 shows the viscosity measured as a function of force for parallel plate rheometry. The measured viscosity for three-point bending was also found

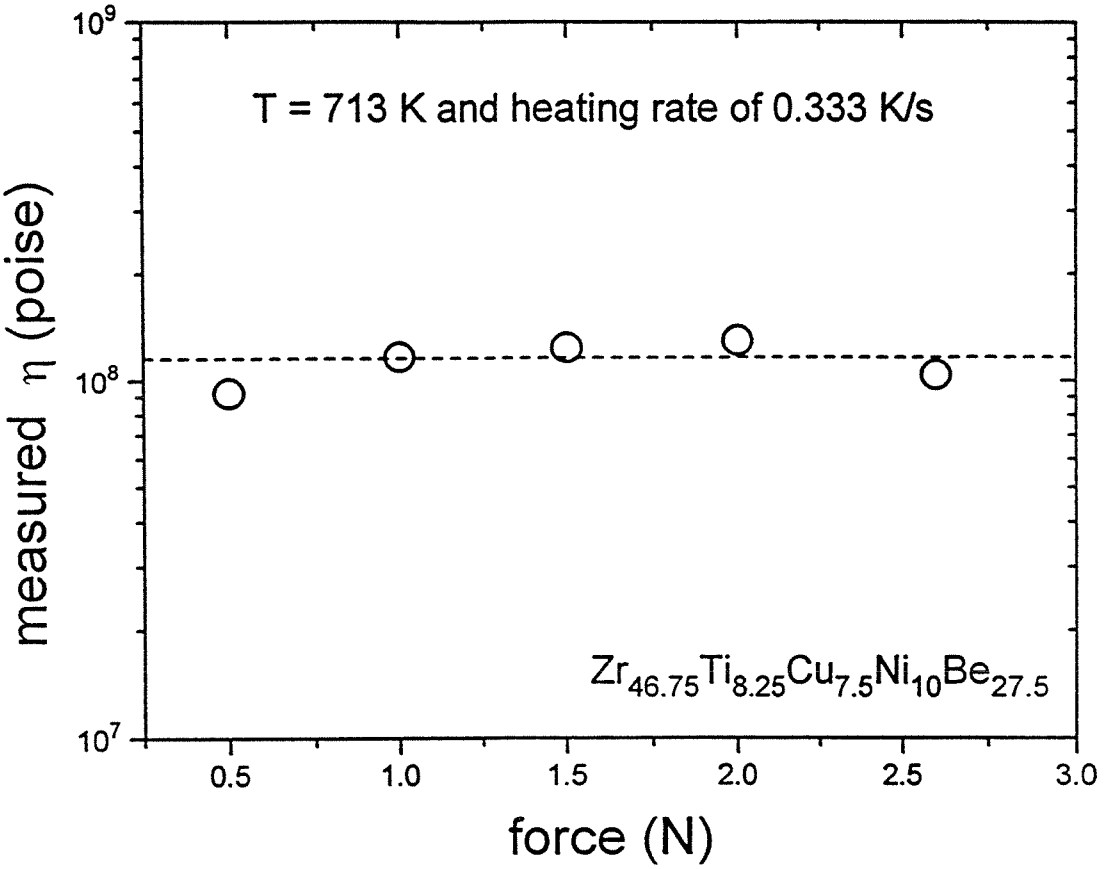

Fig. 5.1. Measured viscosity as a function of force for parallel plate measurements of the $Zr_{46.75}Ti_{8.25}Cu_{7.5}Ni_{10}Be_{27.5}$ alloy at 713 K.

independent of force over the range of measuring forces applied. Independence of measured viscosity with applied force indicates Newtonian viscous flow. However, at these low rates of strain, Newtonian or non-Newtonian character of the material is not conclusive since even non-Newtonian materials can exhibit an approximately linear relationship between stress and strain rate for small strain rates. For a process like slow molding, where strain rates are relatively small, the viscosity as represented here can be directly applied. Using higher strain rates, e.g., extrusion, the Newtonian or non-Newtonian character of the material may have to be taken into account. This provision should be kept in mind throughout the discussion presented in the remainder of this section.

The processes of molding and extrusion are used to form the material to a desired shape. Commercial application of bulk metallic glass can be greatly extended using these methods. As mentioned above, the advantage of these methods is that they can be performed at lower temperature than casting from the melt. The disadvantage is that the initial material must be cast in the glassy state, an added step towards manufacturing a product.

5.1 Molding

In order to examine the molding process, special instrumentation had to be developed for controlled heating of a sample of metallic glass from room temperature up through the glass transition region and for forming

it under pressure in a vacuum or inert environment. The main piece of equipment for this task was a commercially available hydraulic press, the MTP-14, from Tetrahedron Associates, Inc., located in San Diego, California. The press is microprocessor controlled and consists of two platens capable of reaching a temperature of 813 K and a force of 2.13×10^5 N. Support equipment, such as closed loop water cooling and computer interface electronics, and the press itself are described in Appendix III.

The bulk glass investigated in this study is composed of five components; Zr, Ti, Cu, Ni, and Be. Each of these elements forms stable oxides that can cause heterogeneous nucleation of the crystalline phase [1]. Growth of the oxide layer on the surface of bulk glasses has been investigated by Sun et al. [2]. Surface finish is also a concern in production of molded pieces. Oxidation of the bulk glass during processing should therefore be avoided or at least minimized. A vacuum chamber was designed and constructed (Fig. 5.2) to address these considerations. The vacuum chamber was fitted between the platens of the press and the internal heaters of the chamber were controlled by the press microprocessor. The ultimate vacuum was 9×10^{-6} Torr at a temperature of 613 K, the typical processing temperature.

Molding of the bulk metallic glass alloy requires special consideration of the difference of the material's characteristics at low temperature (room temperature), during heating (the non-equilibrium state), and at high temperature, near or above T_g. Also, the characteristics of the mold

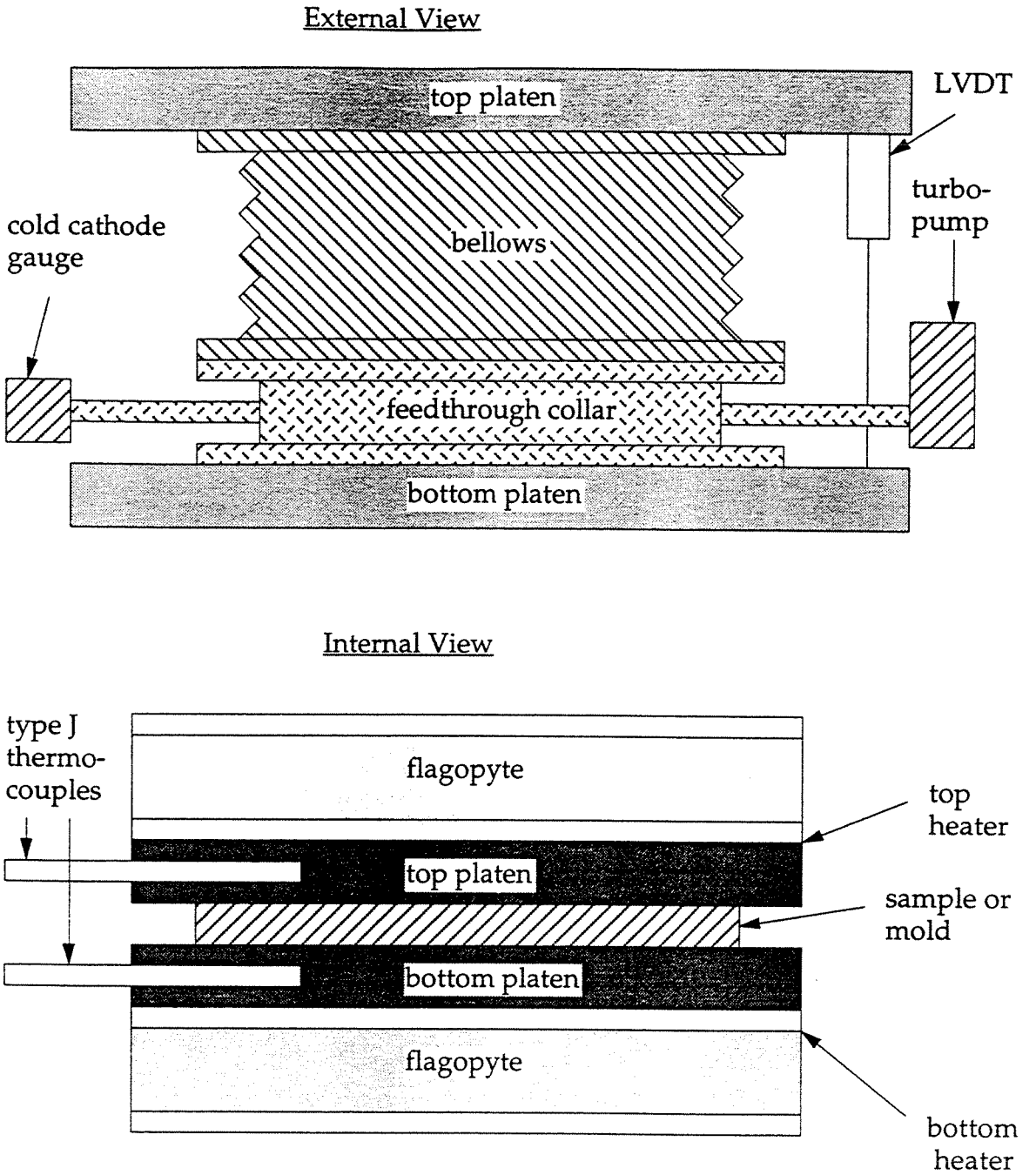

Fig. 5.2. Schematic diagram of the vacuum chamber and internal platens for processing.

material throughout these temperatures have to be chosen carefully. At room temperature, the alloy exhibits a strength of 1.89 GPa and a hardness of 595 kg/mm^2 (54 Rockwell C) [3]. Therefore, one must design the mold such that no force is exerted by the sample onto the mold faces at room temperature. This ensures that fine features to be replicated are not deformed or damaged by the localized high pressure. However, the mold is heated in a vacuum, and the sample must also be heated through thermal conduction, requiring intimate contact. A temperature lag will thus exist between sample temperature and platen temperature. If processed in an inert atmosphere of helium, there would be less difference in sample temperature and platen temperature since helium gas is a relatively good heat conductor. Upon heating, the alloy gradually softens and the viscosity drops dramatically near or above T_g. Here, the mold must maintain its strength in that the sample is a liquid, and all pressures applied to the sample will be transferred hydrostatically to the mold.

Raising the temperature of the metallic glass and the mold over 573 K causes substantial thermal expansion. The linear thermal expansion coefficient of the alloy has been measured to be 9.8 X 10^{-6} /K, roughly half that of steel [4]. A positive or negative feature being replicated can lock the molded piece into the mold due to differential thermal expansion of the two materials. This was discovered upon processing bulk metallic glass completely surrounded by a steel bushing. The resulting flow of the glass

at the elevated temperature filled the free volume, and upon cooling, the steel applies compressive stress, locking the sample into the bushing.

With the above in mind, I designed a two piece mold made of CuBe (Fig. 5.3). This material provides the hardness and the thermal conductivity necessary to obtain optimum molding characteristics. Also, by using this mold in a vacuum, heating rates were larger than heating rates performed in air. By using a higher heating rate, one can take better advantage of the non-equilibrium viscosity of glass during heating for processing purposes. As was shown in Fig. 3.6, Chapter 3, the viscosity during heating can be orders of magnitude lower than the equilibrium value. By applying pressure after the alloy softens (above 573 K), and before the viscosity reaches the equilibrium value, a lower force is required compared to the force required at equilibrium. Fig. 5.4 shows the pressure and temperature profile for a typical molding experiment. A right cylindrical piece of bulk metallic glass (8.4 mm in height by 9.8 mm in diameter) is heated in the mold between the platens at a rate of 20 K/min. Once the sample has reached 580 K, pressure is applied and the sample flows to fill the volume. The time to fill the portion of the mold to be replicated takes about 15 minutes at a temperature of 613 K. The viscosity can only be estimated from the height versus time of this experiment (Fig. 5.5) because the pressure changes as the sample changes its cross sectional area. At this temperature, I estimate a viscosity of 2×10^{11} poise, which is in good agreement for viscosity as measured in Chapter 3. The time for

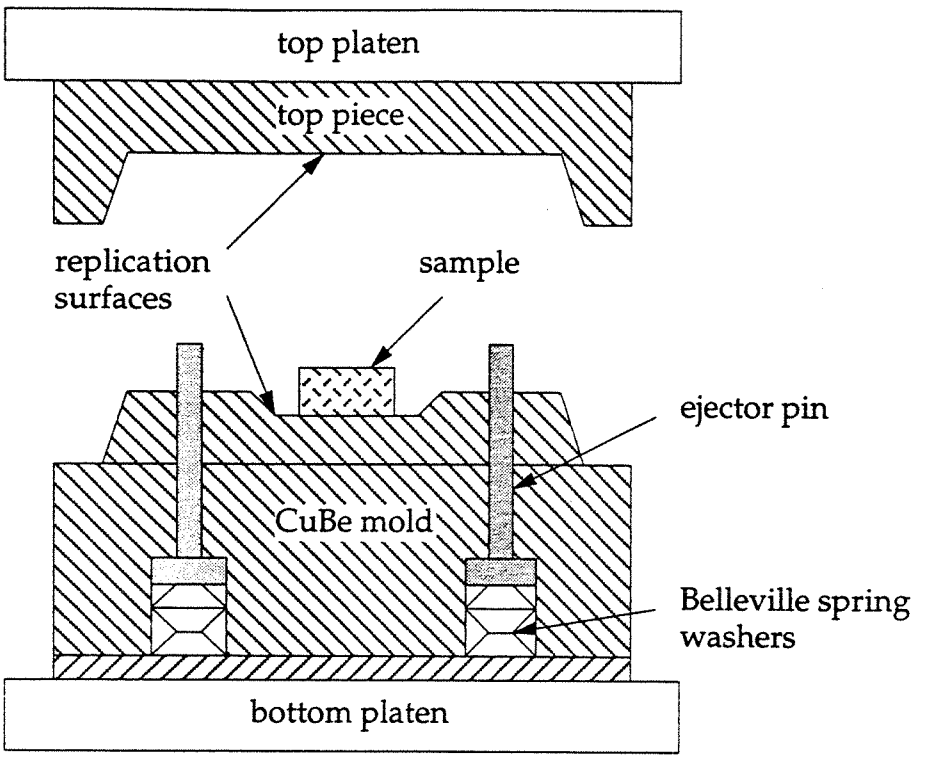

Fig. 5.3. Schematic diagram of the CuBe mold used for processing.

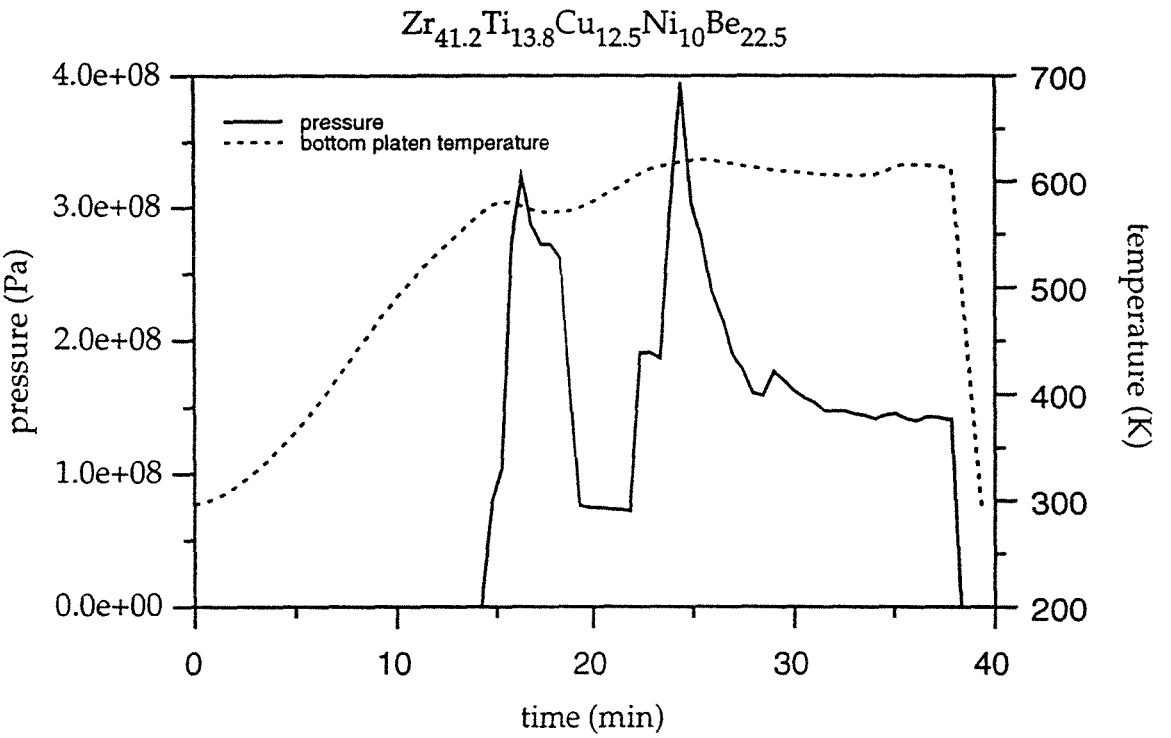

Fig. 5.4. Pressure and temperature profile used to mold the $Zr_{41.2}Ti_{13.8}Cu_{12.5}Ni_{10}Be_{22.5}$ alloy.

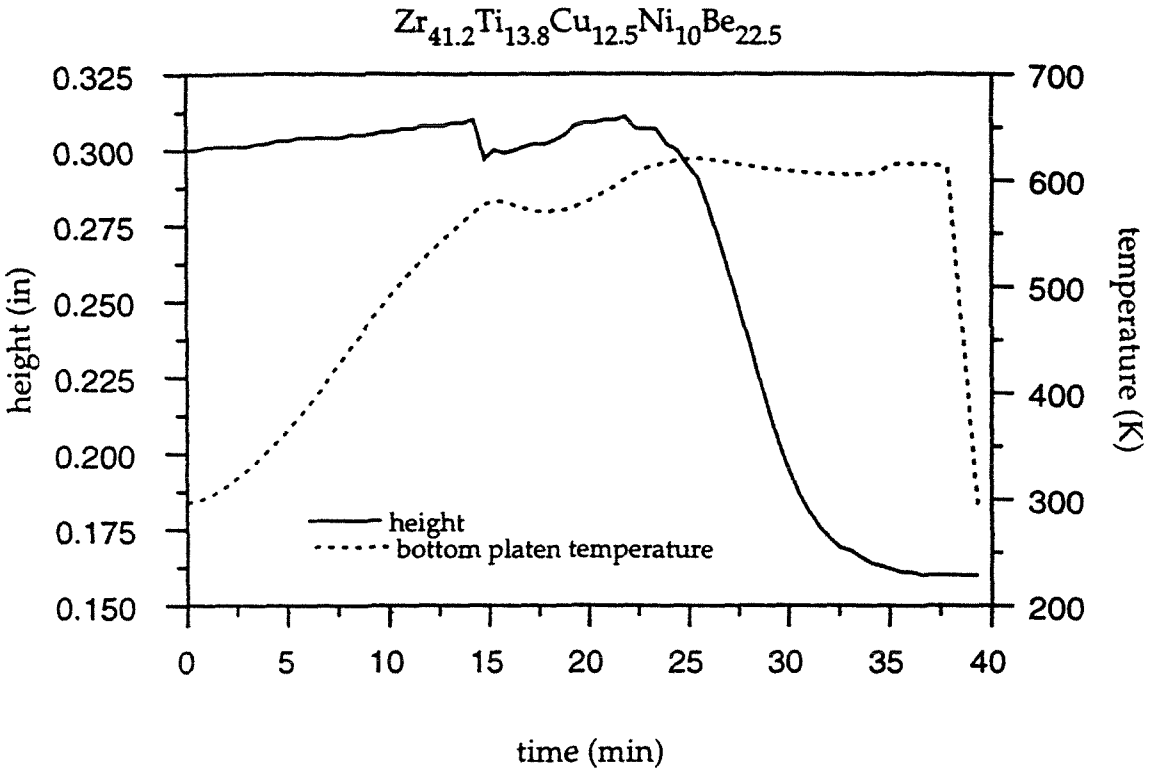

Fig. 5.5. Temperature and height profile used to mold the $Zr_{41.2}Ti_{13.8}Cu_{12.5}Ni_{10}Be_{22.5}$ alloy.

molding will depend on the viscosity of the material, which in turn depends on the processing temperature and the heating rate applied to the sample as discussed above.

The resulting molded pieces are shown in Figs. 5.6 and 5.7, with magnified views of various features. The $Zr_{46.75}Ti_{8.25}Cu_{7.5}Ni_{10}Be_{27.5}$ and the $Zr_{41.2}Ti_{13.8}Cu_{12.5}Ni_{10}Be_{22.5}$ alloys were used. From the magnified views, they are shown to have excellent microformability. The alloys flow into impressions with an accuracy of at least 0.1 micron. The ability of the alloys to flow and match the pattern at these accuracies is also shown by the mechanical bond between the alloys and the pattern on which it is pressed. The mold pattern had machine marks which were transferred to the molded piece. These features can be seen as grooves, hills, and valleys. These result in interlocking of the mold and sample. Even with draft angles of 15°, which is normally self-releasing for most materials, the bulk metallic glass remains locked in the mold. This microformability will have to be taken into account when designing molds for processing the alloy.

5.2 Extrusion

Another method of processing the glass is through extrusion. In the process of extrusion, a piece of material in a stock form, is converted into a continuous length of uniform cross section by forcing it to flow through a die orifice under high pressure. The pressure required will depend on the viscosity of the material, the total reduction in cross sectional area, the rate

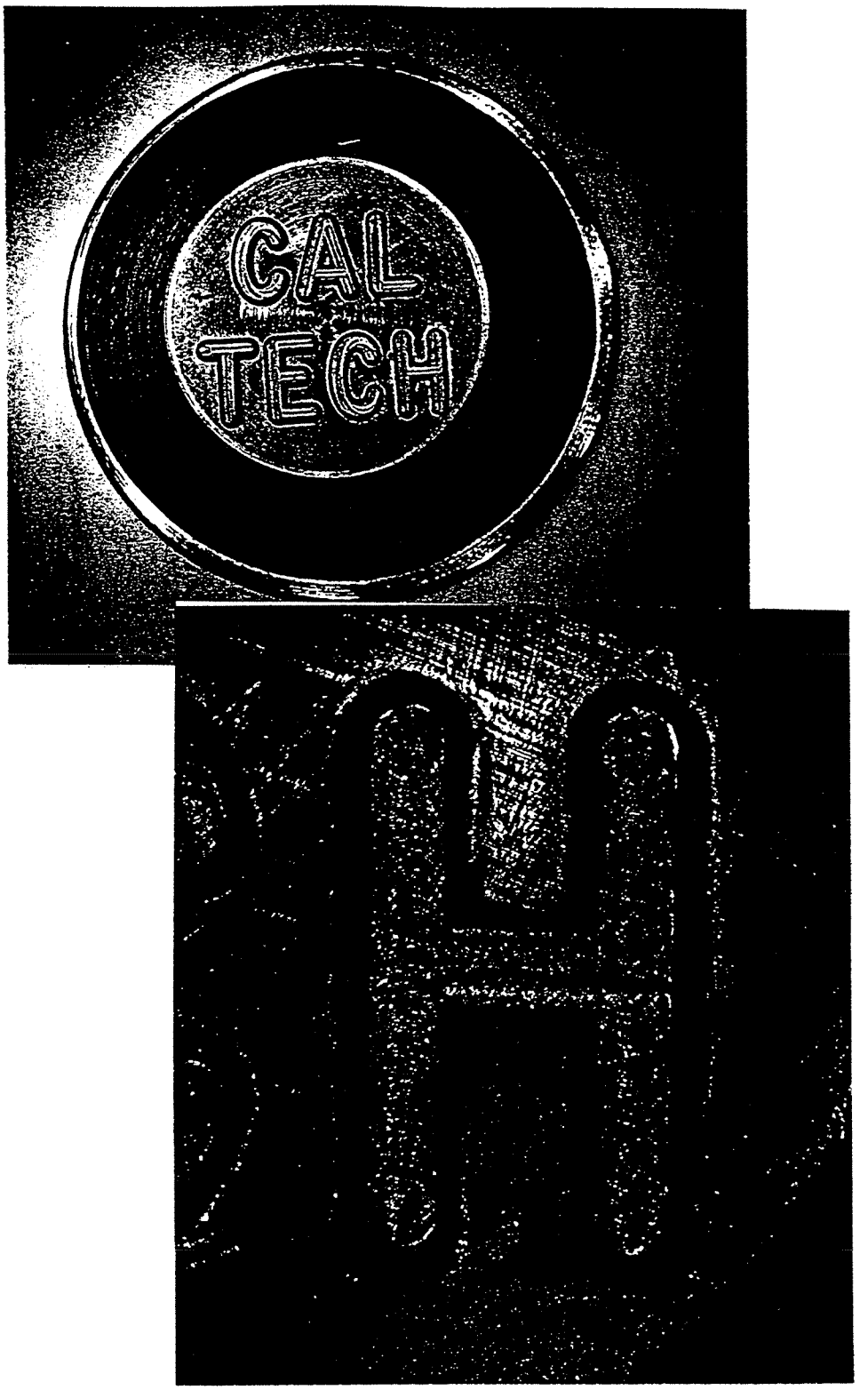

Fig. 5.6. Molded sample of $Zr_{41.2}Ti_{13.8}Cu_{12.5}Ni_{10}Be_{22.5}$ with magnified views of the various features.

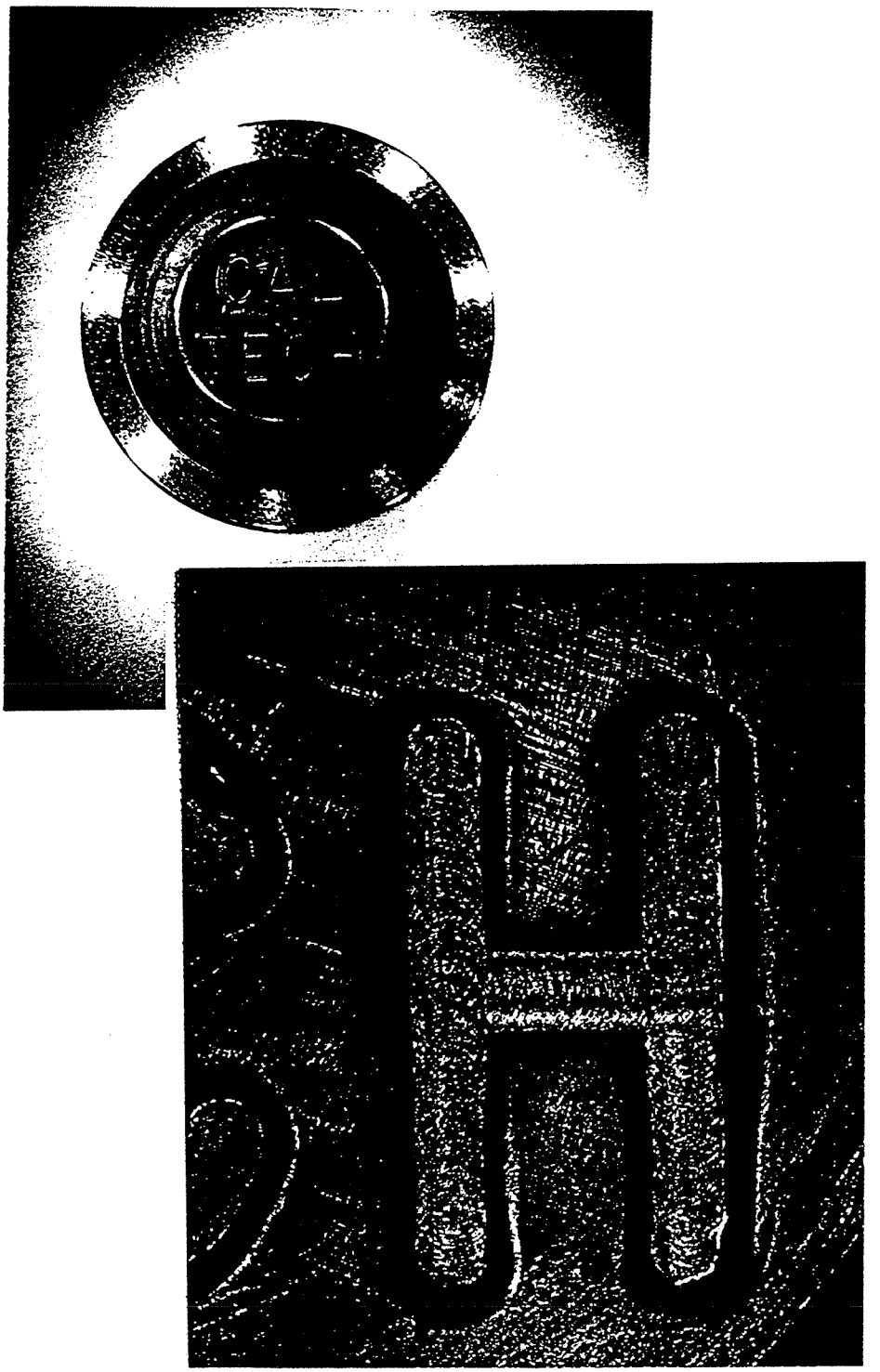

Fig. 5.7. Molded sample of $Zr_{46.75}Ti_{8.25}Cu_{7.5}Ni_{10}Be_{27.5}$ with magnified views of the various features.

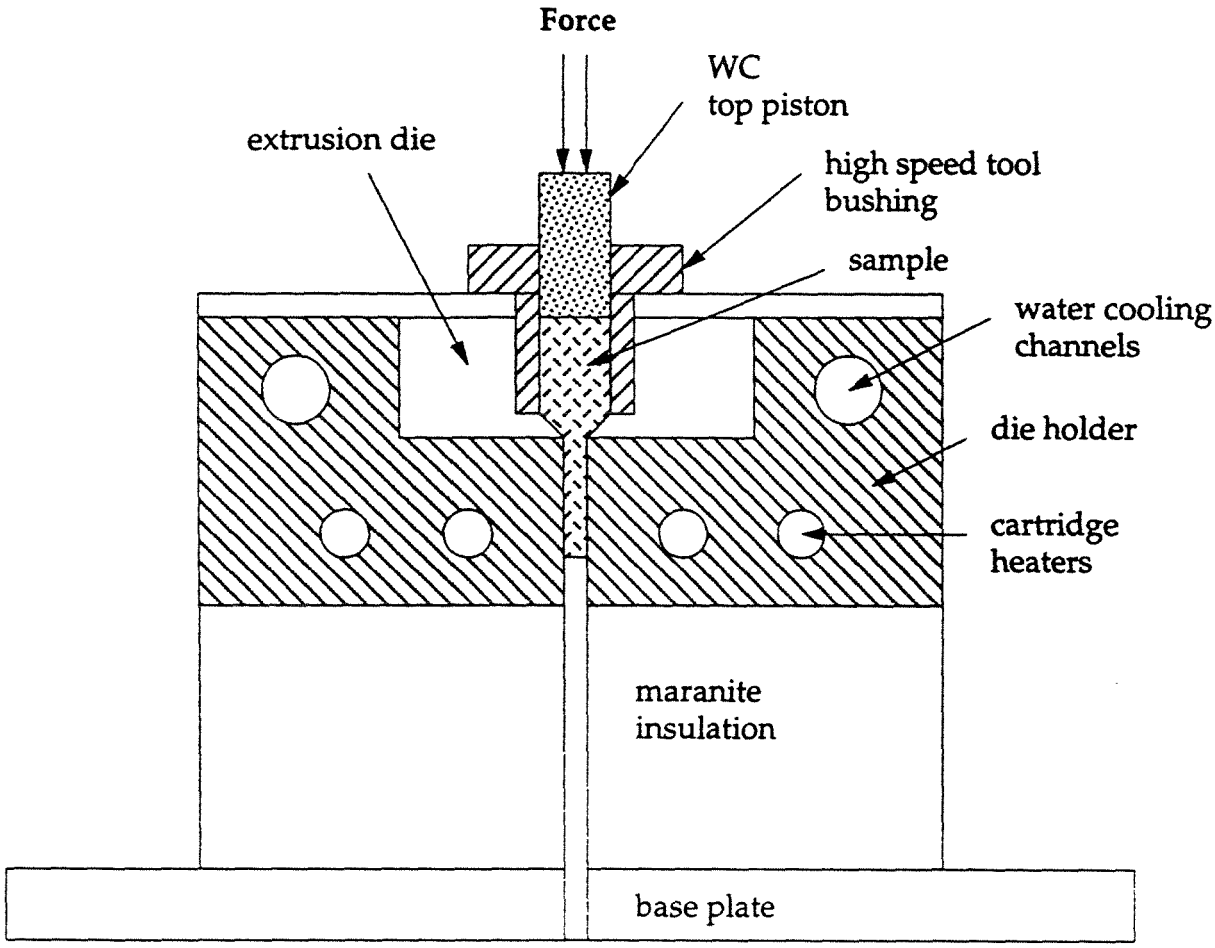

Fig. 5.8. Schematic of extrusion apparatus for processing bulk metallic glass.

of deformation, and on the die shape [5]. Again, because these alloys soften near T_g, and the viscosity falls dramatically with temperature, extrusion is a method very well adapted for processing bulk metallic glasses.

The extrusion apparatus designed for these experiments is shown in Fig. 5.8. Here, a right circular cylinder of the $Zr_{46.75}Ti_{8.25}Cu_{7.5}Ni_{10}Be_{27.5}$ alloy is forced through the extrusion die at elevated temperature for an area reduction of 36 (a 6 mm diameter stock material is extruded into an 1 mm diameter wire). The conditions of the experiment were:

Temperature: heated to 723 K @ 20 K/min

Pressure: 770 MPa

time to complete: 15 minutes

Approximately 7 cm of material was extruded for a total displacement of the stock material of 1.9 cm. At this high temperature, the extruded sample exhibits embrittlement characteristic of partial or complete crystallization. The aggressive area reduction for this experiment, a factor of 36, will have to be reduced so that lower temperatures can be used, which will eliminate the annealing embrittlement. Again, the characteristics of the bulk metallic glass and the extrusion die at all temperatures must be taken into consideration when designing such experiments.

References

[1] X. Lin (Ph.D. thesis in preparation, Califonia Institute of Technology, 1997).

[2] X. Sun, S. Schneider, U. Geyer, W. L. Johnson, and M. A. Nicolet, J. Mat. Res. (in press 1996).

[3] H. A. Bruck, T. Christman, A. J. Rosakis, and W. L. Johnson, Script. Met. **30**, 429 (1994).

[4] Y. He, R. B. Schwarz, and D. G. Mandrus, J. Mat. Res. **11**, (July 1996 issue).

[5] C. E. Pearson and R. N. Parkins, *The Extrusion of Metals*, John Wiley & Sons Inc., New York, 180 (1960).

Chapter 6:

CONCLUSION

The time between discovery of metallic glasses in the form of thin films and their first commercial application as thin ribbons was about 20 years [1]. Since that time, a more systematic approach was taken to 'discover' bulk metallic glasses and find commercial uses for them [2]. As with thin ribbons of metallic glass, bulk metallic glass will also be more than just a scientific curiosity. Commercial uses are already being pursued, and the molding experiments performed in this thesis have made some of this possible. These novel materials, with their mechanical properties as well as their thermal stability, will allow countless future investigations in the area of physical metallurgy and amorphous materials.

The equipment developed in the course of this thesis, specifically the MTP-14 Tetrahedron press, can be used for experiments beyond processes like molding. Of the thermodynamic variables of temperature, pressure and composition, the press system can be used to vary the first two in a controlled, reproducible fashion. The pressure dependence of the glass transition and crystallization of these bulk metallic glasses can be investigated, something for which there is not much data in the existing literature (see Ref. 3, for example).

The methods used to measure viscosity in this thesis have been used to measure glasses like polymers [4] and silicates [5, 6], or the low viscosities

of fluids in the case of capillary flow [7]. Parallel plate requires samples of millimeter or greater dimension. As of a couple of years ago, there were no metallic glasses available of this size. However, with the advent of bulk metallic glass, this method of measuring viscosity has been used for the first time on metallic glass systems. The measurable range of viscosity is now greatly expanded by the high thermal stability in the supercooled liquid of these bulk metallic glasses. Not only can viscosity measurements be extended further into the supercooled liquid, but different methods of viscosity can now be applied.

Measurement of the viscosity dependence with temperature of metallic glass has been shown in this thesis as one way of indicating glass forming ability. The fact that bulk metallic glass fits the prevailing picture of strong glass formers, as compared to other metallic glass systems, is comforting. Measuring viscosity is one way to determine the glass forming ability. Prior to this study, the strong or fragile glass behavior of metallic glass was inconclusive due to the lack of data in the supercooled liquid region. Measurements into this region have shown that our bulk metallic glasses do indeed have strong glass behavior.

The determination of the viscosity of bulk metallic glass as a function of temperature has lead to the knowledge of how these metallic alloys fit into the more general picture of all glass formers:

'Door meten tot weten.'

References

[1] R. Zallen, *The Physics of Amorphous Solids*, John Wiley & Sons Inc., New York, 31 (1983).

[2] W. L. Johnson, *Metals Handbook*, 10th Edn., Vol. 2 ASM International, Metals Park, OH, 812 (1990).

[3] E. G. Ponyatovsky and O. I. Barkalov, Mat. Sci. Rep. **8**, 147 (1992).

[4] G. J. Diennes and H. F. Klemm, Appl. Phys. **17**, 458 (1946).

[5] S. J. Wilson and D. Poole, Mat. Res. Bull. **25**, 113 (1980).

[6] H. E. Hagy, Jour. Am. Ceram. Soc. **46**, 93 (1963).

[7] E. W. Washburn, Phys. Rev. **17**, 273 (1921).

APPENDIX I

The following arguments are from Ref. [AI.1] and Ref. [AII.2] . Starting with the reduced equation of motion:

$$\frac{\partial p}{\partial r} = \eta \frac{\partial^2 v_r}{\partial z^2} \tag{A.I.1}$$

Integrating twice with respect to z and using the boundary conditions:

$$v_r = \frac{1}{2\eta} \frac{\partial p}{\partial r} (z - h) z \tag{A.I.2}$$

The flow through surface element $rd\theta dz$ is $rd\theta v_r dz$. Then U , the flow per unit arc length between the planes $z = 0$ and $z = h$ (in the direction of increasing r):

$$U = \int_0^h v_r dz \quad = -\frac{h^3}{12\eta} \frac{\partial p}{\partial r} \tag{A.I.3}$$

If the plate $z = h$ moves toward the plate at $z = 0$, then the rate of decrease of the volume element must equal the net rate of outward radial flow. Thus;

$$-rdrd\theta \frac{dh}{dt} = \frac{\partial}{\partial r}(rd\theta U)dr \tag{A.I.4}$$

Substitute for U :

$$\frac{12\eta}{h^3}\frac{dh}{dt}r = \frac{\partial}{\partial r}(r\frac{\partial p}{\partial r}) \tag{A.I.5}$$

Integration twice with respect to r gives:

$$p = \frac{3\eta}{h^3}\frac{dh}{dt}r^2 + C^{'}\ln r + C \tag{A.I.6}$$

Since p must be finite for $r = 0$, C' vanishes. C is evaluated at the outer boundary of the specimen, $r = R$, where the pressure must be in equilibrium with the constant pressure P, in this case atmospheric;

$$C = P - \frac{3\eta}{h^3}\frac{dh}{dt}R^2 \tag{A.I.7}$$

which makes the above expression:

$$p = -\frac{3\eta}{h^3}\frac{dh}{dt}(R^2 - r^2) + P \tag{A.I.8}$$

The force can then be written as:

$$F = -2\pi \frac{3\eta}{h^3} \frac{dh}{dt} \int_0^R (R^2 - r^2) r dr \qquad \text{(A.I.9)}$$

Assuming a constant volume between the plates, integration yields:

$$F = -\frac{3\eta V^2}{2\pi h^5} \frac{dh}{dt} \qquad \text{(A.I.10)}$$

Integration with respect to time gives:

$$\frac{1}{h^4} = \frac{8\pi F}{3\eta V^2} t + C'' \qquad \text{(A.I.11)}$$

where C'' is constant of integration. It's value is not important, however since the viscosity is calculable from the slope of $\frac{1}{h^4}$ versus time. This result is for the specimen smaller than the two parallel plates. Solutions for the case where the specimen is larger then the two plates are:

$$F = -\frac{3\pi\eta a^4}{2h^3} \frac{dh}{dt} \qquad \text{(A.I.12)}$$

and

$$\frac{1}{h^2} = \frac{4F}{3\pi\eta a^4} t + C'' \tag{A.I.13}$$

By measuring the height with time, the differential form, equation A.I.12, was used in this study.

References

[AI.1] G. J. Diennes and H. F. Klemm, Appl. Phys. **17**, 458 (1946).

[AII.2] M. J. Stefan, Akad. Wiss. Wien. Math.-Natur. Klasse. Abt. 2. **69**, 713 (1874).

APPENDIX II

As mentioned in Section 2.1, the response of a material can be elastic, viscous or both. The rheological equations that govern a Hookean solid and a Newtonian liquid are analogous. Viscosity is defined by:

$$\dot{\varepsilon} = \frac{\tau}{\eta} \tag{A.II.1}$$

and from classical elasticity:

$$\varepsilon = \frac{\tau}{G} \tag{A.II.2}$$

where τ is the shearing stress, ε the strain and G the shear modulus. The coefficient of viscous traction, λ, is related to the coefficient of viscosity, η, as is the shear modulus is related to the Young's modulus, E , for ideal bodies:

$$\lambda = 3\eta \tag{A.II.3}$$

$$E = 3G \tag{A.II.4}$$

Therefore, it is possible to use solutions obtained for the Hookean solid for the Newtonian liquid by replacing E with λ, and strains or deflections, δ, with strain rates, $\dot{\delta}$ [AII.1]. In order to derive equation 2.15, beam theory for static deflection of elastic beams can be used (see Long [AII.2] and Lamb [AII.3], for example).

A beam of Young's modulus E that is placed between two supports at either end will deform under its own weight, which is considered a continuous load. An external force can also be applied to the center of the beam giving a concentrated load (see Fig. AII.1). The resulting deformation from either of these conditions can be calculated from beam theory. The two assumptions of beam theory are; first, plane sections in the cross section of the beam remain plane after deformation, and second, only normal stresses arise on each cross section. This results in the Bernoulli-Euler law:

$$M_B = -\frac{EI_c}{r} \tag{A.II.5}$$

where M_B is the bending moment, I_c the moment of inertia of the cross section, and r is the radius of curvature. The deflection of the beam, δ, is from:

$$\frac{d^2\delta}{dx^2} = -\frac{1}{r} \tag{A.II.6}$$

Combining this with eq. A.II5:

$$EI_c \frac{d^2\delta}{dx^2} = M_B \tag{A.II.7}$$

Using the bending moments as described in Fig. AII.1, this equation can be integrated using the following boundary conditions: $\frac{d\delta}{dx} = 0$ at $x = L/2$ and $\delta = 0$ at $x = 0$. The maximum deflection for a continuous load is:

$$\delta_{\max} = \frac{5mgL^3}{384EI_c} \tag{A.II.8}$$

$$M_B = \frac{1}{2} mg\left(x - \frac{x^2}{L}\right)$$

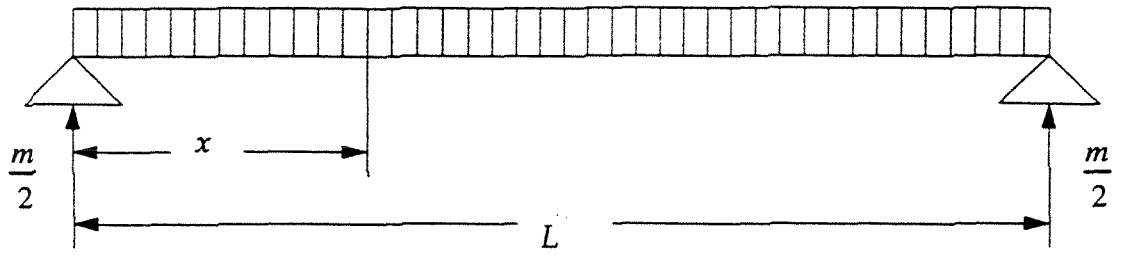

continuous load

m is the mass of the rod between the supports

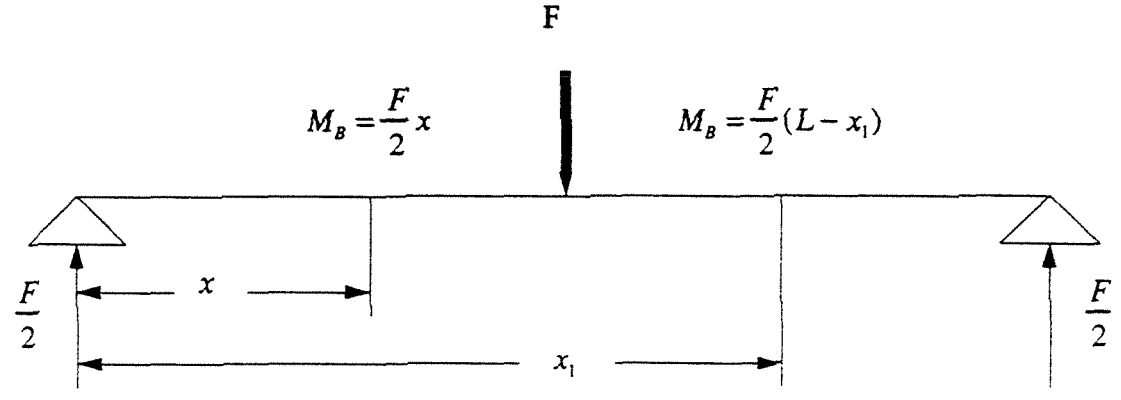

concentrated load at the center

Fig. AII.1. Cases of continuous and concentrated loads and their respective bending moments in three-point bending of a beam.

and for a concentrated load at the center:

$$\delta_{max} = \frac{MgL^3}{48EI_c} \qquad \text{(A.II.9)}$$

Since the above equations are linear, the deflection of a beam from different loading systems may be added, for a total deflection of:

$$\delta_{max} = \frac{gL^3}{48EI_c}\left(M + \frac{5m}{8}\right) \qquad \text{(A.II.10)}$$

By using the substitutions mentioned above, this can be rewritten for the flow at the center of a beam with a load placed at the center:

$$\eta = \frac{gL^3}{144I_c\delta_{max}}\left(M + \frac{5m}{8}\right) \qquad \text{(A.II.11 or 2.15)}$$

References

[AII.1] M. Reiner, *Rheology*, Vol. 1 (ed F. R. Eirich), Academic Press, New York, 9 (1956).

[AII.2] R. R. Long, *Mechanics of Solids and Fluids*, Prentice-Hall, Inc., Englewood Cliffs, N. J., 91 (1961).

[AII.3] H. Lamb, *Statics*, Cambridge University Press, London, 312 (1921).

APPENDIX III

The MTP-14 press, as received from the manufacturer, Tetrahedron Associates, Inc., San Diego, California, has the following capabilities:

	Minimum	Maximum
Force:	500 lbs (2.2×10^3 N)	48000 lbs (2.13×10^5 N)
Temperature:	ambient	1000 F (540 C)
Heat Rate:	0 F/min (0 C/min)	15 F/min (8 C/min)
Quench Rate:	0 F/min (0 C/min)	400 F/min (220 C/min)

Area of platens: 14 in x 14 in (36 cm x 36 cm)

Temperature uniformity @ 350 F: (177 C) is +/- 5 F (3 C).

Height gauge reads from + 0.500 in to -0.500 in +/- 0.001 in.

Daylight is variable from 6 in (15.24 cm) to 12 in (30.5 cm).

A schematic of the press structure is shown in Fig. AIII.1. The press has an on-board microprocessor and all its functions can be programmed. During the course of my research, I found it more convenient to operate the press manually (except water cooling). This would not be the case if used in production. Operation of the press required development of support equipment.

A closed loop cooling system for bolster cooling and quenching of the main platens was designed. It consisted of two water pumps, each dedicated to the above tasks. The pumps can be manual or automatically controlled. For the purposes of this study, water cooling was always done

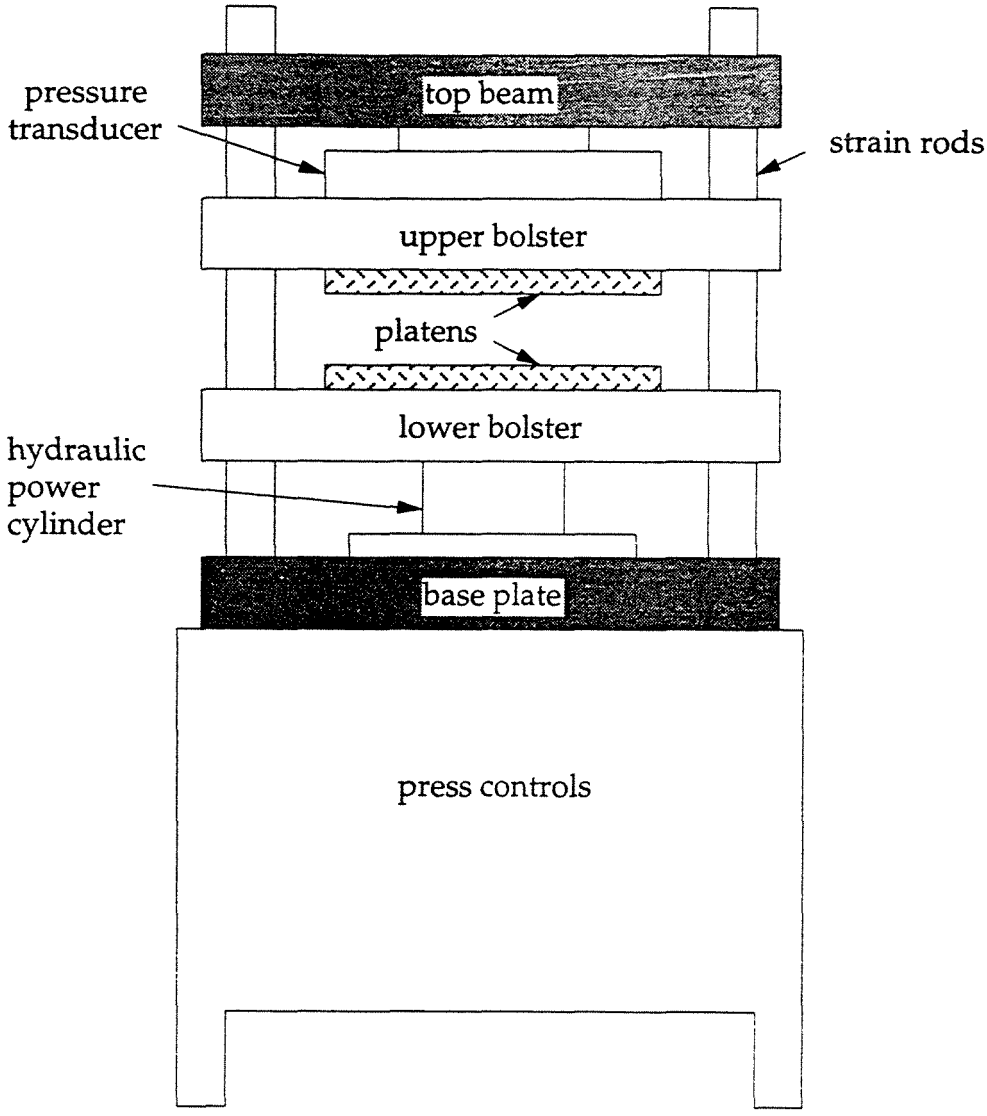

Fig. AIII.1. Schematic diagram of the MTP-14 press structure.

automatically. In the auto mode, magnetic starters to the pumps are switched on by relays controlled by the press microprocessor for different temperature settings. The temperature is monitored by four type J thermocouples in two zones on each platen. Planar heaters, two per platen, ensure uniform temperature over the large area of the platens.

During quenching, 12 gallons of water/ethylene glycol per minute at room temperature is passed through cooling channels in the platens for a maximum cooling rate of 220 K/min. The exiting cooling fluid is then cooled in a heat exchanger. The heat exchanger consists of copper tubes coaxially welded into a stainless cylinder which has two gallons of industrial water per minute flow. Although not 100% efficient, the 55 gallon reservoir of cooling fluid doesn't reach boiling after continuous use, which would be the case if there were no heat exchanger. The four cooling lines from the platen have pressure relief valves at the bolster and check valves after the heat exchanger to prevent damage to the connecting hoses. A schematic of the MTP-14 press system is shown in Fig. AIII.2.

The microprocessor performs diagnostics of the press parameters and compares them to the set points at a rate of twice per second. This limits the response time of the press to achieve the proper setting. For example, initial closing of the press and application of the set force is limited by the pressure transducer response time. No matter what the initial setting, the force rises sharply then reaches an equilibrium value. This rise in force is approximately 3 klbs (1.3×10^4 N). As mentioned in Chapter 5, this has to

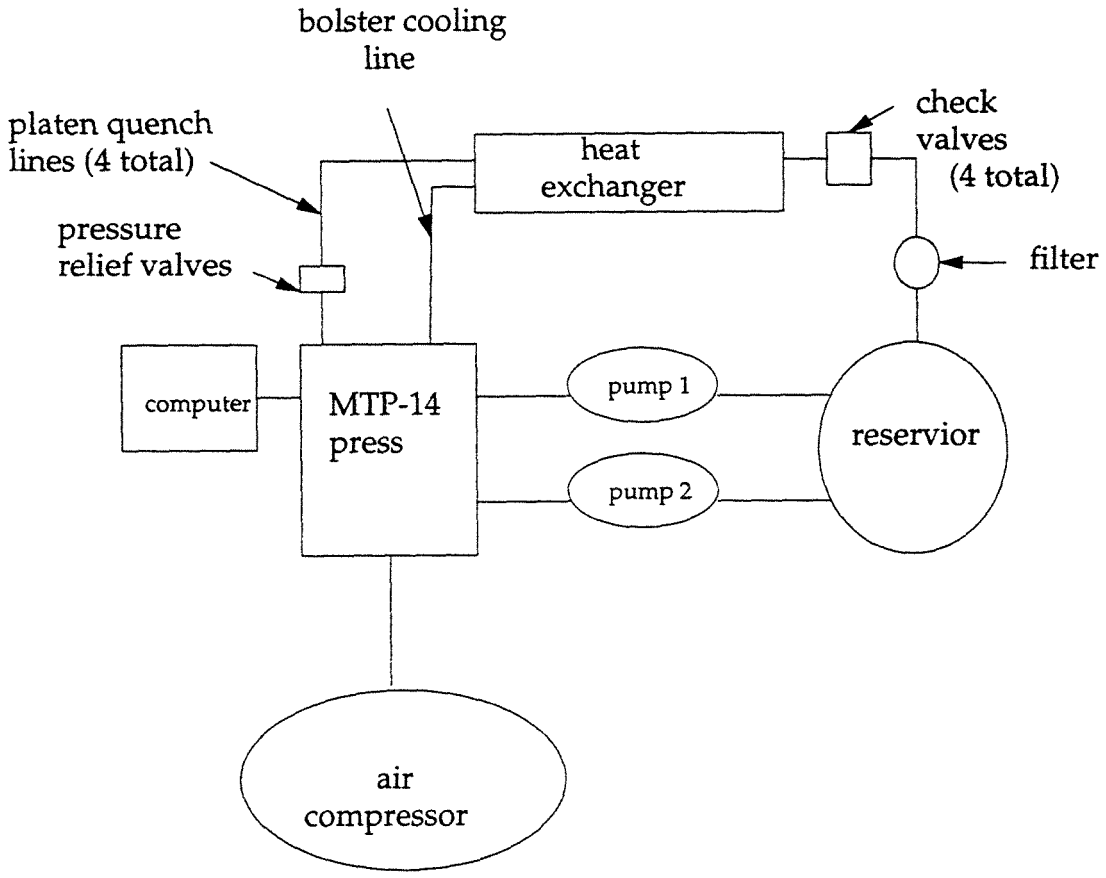

Fig. AIII.2. Schematic diagram of the press system.

be taken into consideration when designing molds in that fine features will be deformed should this force be too high.

The press has a RS-232 output labeled 'Digigraph' which can be used to record all parameters of the operation via an external computer. Again, the diagnostics are performed twice per second, and information will only be exported at a maximum rate of once per second. The parameters are formatted in standard ASCII characters and can be read serially by any number of software packages. I chose to use Windows® port communication, and transfer data to another spreadsheet for analysis.

Initial molding experiments were done exposed to atmosphere. Later experiments, to avoid oxidation, a vacuum chamber was designed (see Fig. 5.2) in which force provided by the platens was transferred through the bellows. This system has two internal platens heated by planar heaters which are nichrome ribbon sandwiched between two layers of Flagopyte. The heater/platen system is insulated from the rest of the press by 2 cm of layered Flagopyte. Since the heating system is in a vacuum under high pressure and temperature, choice of material is limited. Flagopyte layers were chosen because they are fracture tough, thermally insulating, and have reduced outgassing (compared to most ceramics). Platen temperature was monitored by type J thermocouples and temperature was controlled by the press microprocessor.

The planar heaters used in a vacuum are ribbon nichrome. Usually, wire nichrome imbedded in a ceramic is used in atmosphere. Since the

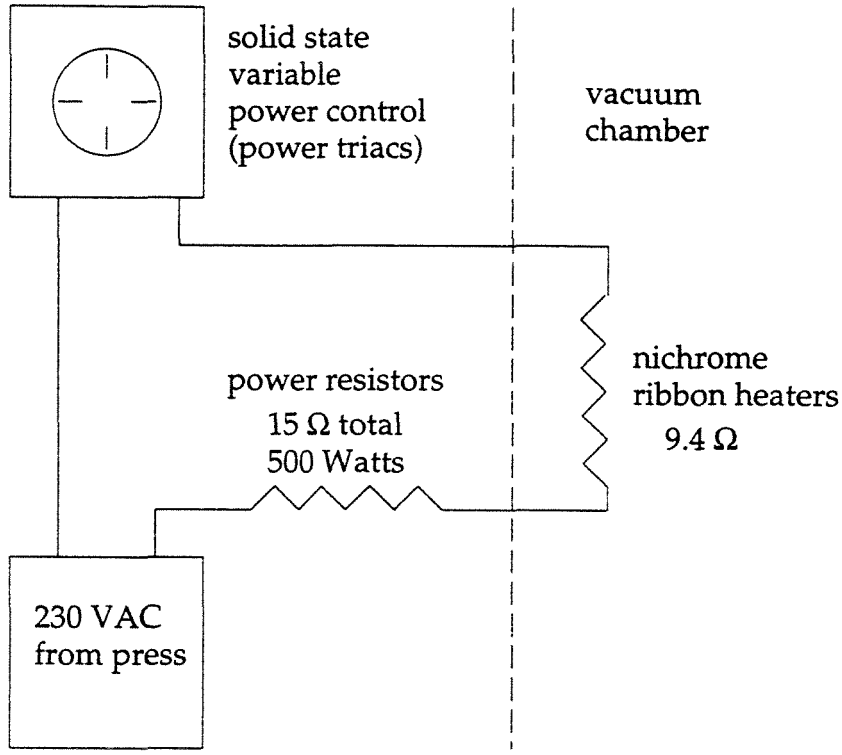

Fig. AIII.3. Voltage control for the nichrome ribbon heaters, one for each platen (top and bottom).

press was used for heater control, the lower resistance of ribbon heaters is taken into account by using external voltage transformers (see Fig. AIII.3). Once the sample had been heated and formed, it was removed from the vacuum system and water quenched in atmosphere. Most oxidation of the processed sample occurred only during this step of the process.